

## Characteristics and Predictability of Midwestern United States Drought

ANDREW HOELL,<sup>a</sup> TRENT W. FORD,<sup>b</sup> MOLLY WOLOSZYN,<sup>c,d</sup> JASON A. OTKIN,<sup>e</sup> AND JON EISCHEID<sup>d,a</sup>

<sup>a</sup> NOAA/Physical Sciences Laboratory, Boulder, Colorado

<sup>b</sup> Illinois State Water Survey, Prairie Research Institute, University of Illinois Urbana–Champaign, Champaign, Illinois

<sup>c</sup> NOAA/National Integrated Drought Information System, Boulder, Colorado

<sup>d</sup> Cooperative Institute for Research in the Environmental Sciences, University of Colorado Boulder, Boulder, Colorado

<sup>e</sup> Space Science and Engineering Center, Cooperative Institute for Meteorological Satellite Studies, University of Wisconsin–Madison, Madison, Wisconsin

(Manuscript received 9 March 2021, in final form 29 September 2021)

**ABSTRACT:** Characteristics and predictability of drought in the midwestern United States, spanning from the Great Plains to the Ohio Valley, at local and regional scales are examined during 1916–2015. Given vast differences in hydroclimatic variability across the Midwest, drought is evaluated in four regions identified using a hierarchical clustering algorithm applied to an integrated drought index based on soil moisture, snow water equivalent, and 3-month runoff from land surface models forced by observed analyses. Highlighting the regions containing the Ohio Valley (OV) and Northern Great Plains (NGP), the OV demonstrates a preference for subannual droughts, the timing of which can lead to prevalent dry epochs, while the NGP demonstrates a preference for annual-to-multiannual droughts. Regional drought variations are closely related to precipitation, resulting in a higher likelihood of drought onset or demise during wet seasons: March–November in the NGP and all year in the OV, with a preference for March–May and September–November. Due to the distinct dry season in the NGP, there is a higher likelihood of longer drought persistence, as the NGP is 4 times more likely to experience drought lasting at least one year compared to the OV. While drought variability in all regions and seasons is related to atmospheric wave trains spanning the Pacific–North American sector, longer-lead predictability is limited to the OV in December–February because it is the only region/season related to slow-varying sea surface temperatures consistent with El Niño–Southern Oscillation. The wave trains in all other regions appear to be generated in the atmosphere, highlighting the importance of internal atmospheric variability in shaping Midwest drought.

**SIGNIFICANCE STATEMENT:** The midwestern United States, spanning from the Great Plains to the Ohio Valley, has endured many costly and life-altering droughts. A drought in 2012 led to an estimated \$34.5 billion in direct economic losses. This study aims to build a more complete understanding of drought in regions of the Midwest that could be used in drought early warning efforts. Drought is evaluated in four midwestern regions of coherent hydroclimatic variability. The regions were identified by applying a method that groups similar objects to an integrated drought index that includes soil moisture, snow water equivalent, and 3-month runoff from land surface models during 1916–2015. Highlighting the regions containing the Ohio Valley (OV) and Northern Great Plains (NGP), droughts in the NGP generally last longer than in the OV. Droughts in the NGP only begin and end during the warm and wet season while droughts in the OV can begin and end during any time of year. El Niño–Southern Oscillation (ENSO), a slow varying phenomenon of the Earth system, may be used as a source of predictability for drought onset and demise in the OV during winter. However, circulation patterns internal to the atmosphere play a key role in shaping drought in all other seasons and regions of the Midwest.

**KEYWORDS:** Drought; Climate variability; ENSO; Trends

### 1. Introduction

Drought is a natural and recurring feature of midwestern United States hydroclimate (Diaz 1983; Englehart and Douglas 2003) and has meaningful effects on the region's socioeconomic well-being. The definition of the midwestern United States, referred to as the Midwest and shown in Fig. 1a, is taken from the U.S. Census Bureau (2021). Kentucky is also included because it is part of the Midwest Drought Early Warning System (National Integrated Drought Information System 2021). As part of the “Corn Belt” in the United States (U.S. Department of Agriculture National Agricultural Statistics

Service 2019) and one of the most agriculturally productive areas in the world (Oppedahl 2018; U.S. Department of Agriculture Midwest Climate Hub 2021), the Midwest produces less for consumption and export during drought (Mishra and Cherkauer 2010; Lobell et al. 2014). During the 2012 drought, for example, the United States lost about one quarter of its corn and sorghum production (Rippey 2015). Also, rivers are an important mode of transportation in the Midwest, and because drought lowers water levels in key rivers like the Mississippi, Illinois, and Ohio, barges must transport lighter loads to not run aground (State of Illinois Department of Natural Resources 2013). This impacts commodity transportation costs and puts downward pressure on crop prices paid to producers. Drought can also affect human health by reducing drinking water quality and promoting the

Corresponding author: Andrew Hoell, andrew.hoell@noaa.gov

DOI: 10.1175/JHM-D-21-0052.1

© 2021 American Meteorological Society. For information regarding reuse of this content and general copyright information, consult the AMS Copyright Policy ([www.ametsoc.org/PUBSReuseLicenses](http://www.ametsoc.org/PUBSReuseLicenses)).

Brought to you by U.S. Department Of Commerce, Boulder Labs Library | Unauthenticated | Downloaded 11/09/21 07:16 PM UTC

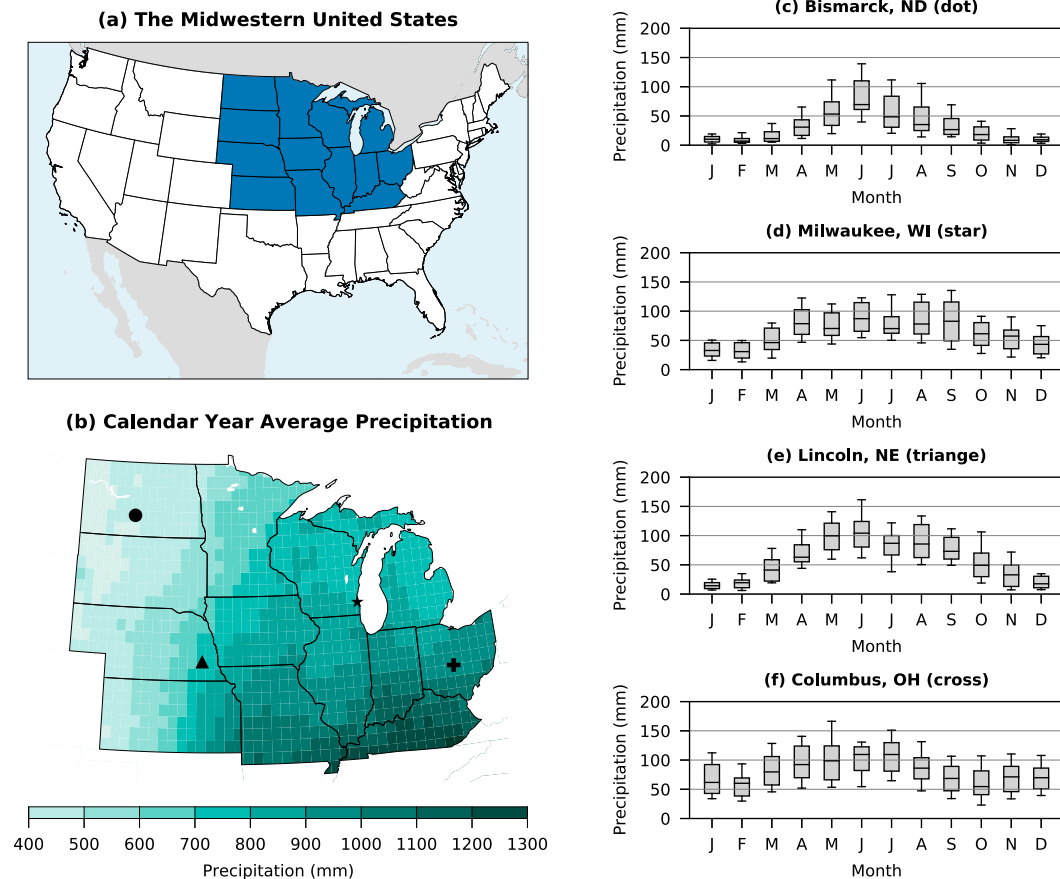


FIG. 1. (a) The U.S. Midwest, defined by the U.S. Census Bureau, and Kentucky. (b) 1916–2015 calendar year average precipitation. (c)–(f) Boxplots of monthly precipitation during 1916–2015 for the grid box containing each location. For the boxplots, whiskers denote the interdecile range, boxes the interquartile range, and the horizontal line the median.

spread of disease by pests such as mosquitoes (Centers for Disease Control and Prevention 2020).

A holistic understanding of the characteristics and predictability of Midwest drought would equip forecasters and planners with the knowledge to better anticipate and prepare for future events. However, studies that have attempted to generalize drought characteristics have not specifically focused on the Midwest (Fig. 1), but rather on continental-scale features spanning the United States or North America. The earliest studies on continental-scale drought characteristics focused on spatial and temporal drought signatures. Drought was found to persist for longer in the interior of the United States than along the coasts (e.g., Klugman 1978; Walsh et al. 1982; Karl and Koscielny 1982; Karl 1983; Diaz 1983; Soulé 1992; Mo and Schemm 2008). However, despite the generalization of longer drought persistence over parts of the central United States, Oladipo (1986) found that drought is largely spatially incoherent over the region and individual drought events rarely affect the entire region at the same time. Early studies on drought onset and demise found that they tend to occur during climatological rainy seasons (Diaz 1983), and portions of those seasons when the heaviest precipitation is

most likely (Karl et al. 1987). Moreover, Mo (2011) found that for much of the United States, drought onset generally takes longer than drought demise because precipitation deficits must accumulate for drought onset whereas just a few rain events can usher drought demise. This generalization, however, does not apply to a class of droughts called flash droughts, whose onsets happen over the course of sub-seasonal time scales amid a myriad of simultaneous weather and climate extremes, including below-average precipitation, warmer-than-average temperatures, and above-average atmospheric moisture demand (Otkin et al. 2018; Pendergrass et al. 2020).

Likewise, studies on drought predictability have largely focused on synoptic to continental-scale patterns and the roles played by the Pacific, and to a lesser degree, the Atlantic Oceans. Early studies established the relationship between sea surface temperature (SST) anomalies and United States drought through statistical associations (e.g., Namias 1983). Tropical Pacific SST anomalies associated with El Niño–Southern Oscillation (ENSO) are related to precipitation across the United States (e.g., Ropelewski and Halpert 1986) and have therefore been linked to drought (e.g., Kahya and Dracup 1993;

Piechota and Dracup 1996; Rajagopalan et al. 2000; Ryu et al. 2010). While many widespread U.S. droughts occurred during the cold phase of ENSO, La Niña (Mo and Lettenmaier 2018), Englehart and Douglas (2003) note that “past drought episodes have not been strongly or simply tied to the ENSO signal.” More recently, studies have examined the predictability of drought in initialized forecast systems like the North American Multimodel Ensemble (Kirtman et al. 2014). Over the United States, Mo et al. (2012) and Mo and Lyon (2015) found that models that realistically simulated drought captured a realistic ENSO response. Globally, Yuan and Wood (2013) found that fewer than 30% of global droughts were detected by forecast models, and that the misses were over regions with low potential predictability due to a weak relationship to ENSO.

It is also important to note that aspects of individual significant drought events have been examined in some depth. However, while the lessons learned from these case studies contribute to our collective knowledge of drought characteristics and predictability, they may lack the generality necessary to be applied to develop comprehensive drought early warning. Notable events affecting the Midwest, among other regions, that have garnered considerable attention include events in the 1930s (e.g., Schubert et al. 2004; Seager et al. 2008), 1950s (e.g., Barlow et al. 2001), 1988 (e.g., Trenberth et al. 1988; Chen and Newman 1998), 2000 (e.g., Seager 2007), and 2012 (e.g., Mallya et al. 2013; Kam et al. 2014; Hoerling et al. 2014), the most recent of which led to economic losses that were estimated at \$34.5 billion (NOAA/National Centers for Environmental Information 2021).

Here, we examine the characteristics and predictability of drought in the Midwest at local and regional scales (Fig. 1). We adapt the methodology of Mo and Lettenmaier (2018), which quantified drought using an integrated drought index (IDI) derived from four land surface model simulations forced by estimates of the time varying meteorology spanning 1916–2015. This IDI is based on total moisture storage, which itself is defined as the sum of column integrated soil moisture and snow water equivalent, and 3-month runoff. We chose to use this IDI for our study because it includes different facets of drought that are important in the Midwest: agricultural (Wang et al. 2016; Eeswaran et al. 2021), snow (Huning and AghaKouchak 2020), and hydrological (Wang et al. 2011; Poshtiri and Pal 2016).

Our objective is to build a more complete understanding of drought over the Midwest that may be used for effective early warning. In line with past studies (e.g., Oladipo 1986), we find that hydroclimate varies greatly across the Midwest, which suggests that examinations of drought in this region should adopt a local to subregional perspective. We adopt such a perspective, and for the first time, separate the Midwest into four spatially coherent regions of hydroclimatic variability based on a hierarchical cluster analysis of the IDI. We then probe the characteristics and predictability of drought within the four regions by examining the intensity, persistence, and variability of the IDI and identifying related large-scale oceanic and atmospheric conditions that may serve as sources of predictability for drought

events. Specifically, we investigate when regional droughts begin, how long they last, how quickly drought severity can vary, and whether physical factors like ENSO and related atmospheric circulations are associated with drought, potentially rendering them more predictable.

An outline of the article is as follows. In section 2, we describe the methods and tools employed. In section 3, we describe the results, beginning with an assessment of hydroclimatic variations across the Midwest and ending with an examination of the characteristics of drought in regions of the Midwest identified through a cluster analysis of the IDI. In section 4 we provide a summary and in section 5 discuss the conclusions.

## 2. Methods and tools

### a. Land surface models

Four land surface models are analyzed monthly on the same fixed  $0.5^\circ \times 0.5^\circ$  latitude–longitude grid during 1916–2015. They are VIC version 4.0.6 (Liang et al. 1994), Noah version 2.7 (Ek et al. 2003), SAC-SMA (Burnash et al. 1973), and Catchment (Koster et al. 2000; Ducharme et al. 2000). We summarize key aspects of the land surface models relevant to our experimental design and refer readers to Mo and Lettenmaier (2018) and references therein for further details on the models, their differences, and the persistence time scales of variables. All four land surface models were forced using the same estimates of the time-varying meteorology: daily precipitation, wind speed, average temperature, water vapor pressure, and downward solar and longwave radiation. Precipitation and maximum and minimum temperature forcing grids were computed from station data (Wang et al. 2009). Wind speed after 1950 was based on the NCEP–NCAR Reanalysis version 1 (Kalnay et al. 1996). Wind speed before 1950 was based on seasonal averages, which was shown to have little effect on the hydrologic variables (Livneh et al. 2013). Daily average temperature, vapor pressure, and downward solar and longwave radiation were derived from daily precipitation and maximum and minimum temperature, as described by Bohn et al. (2013).

### b. Integrated drought index (IDI)

We quantify drought, or hydroclimate more generally, using an IDI derived from the four historical land surface model simulations. Our IDI is based on the same two quantities as Mo and Lettenmaier (2018): 1) total moisture storage at the surface, which is the sum of column integrated soil moisture and snow water equivalent, and 2) 3-month runoff. Our reasons for including these land surface quantities are threefold. First, an IDI that includes soil moisture, snow water equivalent, and runoff integrates the effects of different facets of drought that are important in the Midwest. It is important to note that an IDI can be constructed using different hydroclimatic variables relevant to different regions; for example, Shah and Mishra (2020) constructed an IDI based on precipitation, soil moisture, and runoff for monitoring drought in India. Second, century-long land surface model simulations allow us to better identify robust drought characteristics than if we were

TABLE 1. A comparison of how our IDI compares to that of [Mo and Lettenmaier \(2018\)](#).

Step	Our IDI	<a href="#">Mo and Lettenmaier (2018)</a>
1	Standardize monthly total moisture storage in each of the four models	Compute monthly total moisture storage percentiles in each of the four models
2	Standardize 3-month runoff in each of the four models	Compute 3-month standardized runoff percentiles in each of the four models
3	Calculate the unweighted monthly mean of the eight total moisture and runoff indices	Calculate the unweighted monthly mean of the eight total moisture and runoff indices
4	Standardized the unweighted monthly grand mean	Transform the unweighted monthly grand mean to a uniform cumulative probability distribution

to use in situ data or other land data assimilation systems that may be spatially incomplete and/or span shorter time periods. Third, utilizing output from several land surface models limits the effects of biases introduced by a single model.

Though our IDI is also based on total moisture storage and 3-month runoff, the way in which it is calculated differs from [Mo and Lettenmaier \(2018\)](#). Our IDI employs only standardized departures whereas the IDI of [Mo and Lettenmaier \(2018\)](#) transforms some variables to a uniform distribution ([Table 1](#)). We use standardized departures to better capture the variability than is possible using uniform distributions. The computation of our IDI follows a four-step process. First, monthly total moisture storage standardized departures were calculated for each of the four models. Second, for each month, 3-month standardized runoff departures were calculated for each of the four models. Third, the unweighted monthly mean of the four

standardized total moisture and four standardized runoff indices was calculated. Finally, standardized departures of the unweighted monthly means were calculated. The calculation of monthly standardized anomalies follows [Shukla and Wood \(2008\)](#), which employed the framework developed by [McKee et al. \(1993\)](#). Variables are fitted to a gamma distribution, followed by a transformation to a normal distribution with a mean of zero and a unit variance. A 1916–2015 monthly reference was used.

### c. Drought characteristics and predictability

We examine the characteristics and predictability of Midwest drought at local and regional scales during 1916–2015. For the local scale, we examine drought characteristics for each grid box to assess spatial variations of hydroclimate across the Midwest. For the regional scale, we examine drought characteristics over

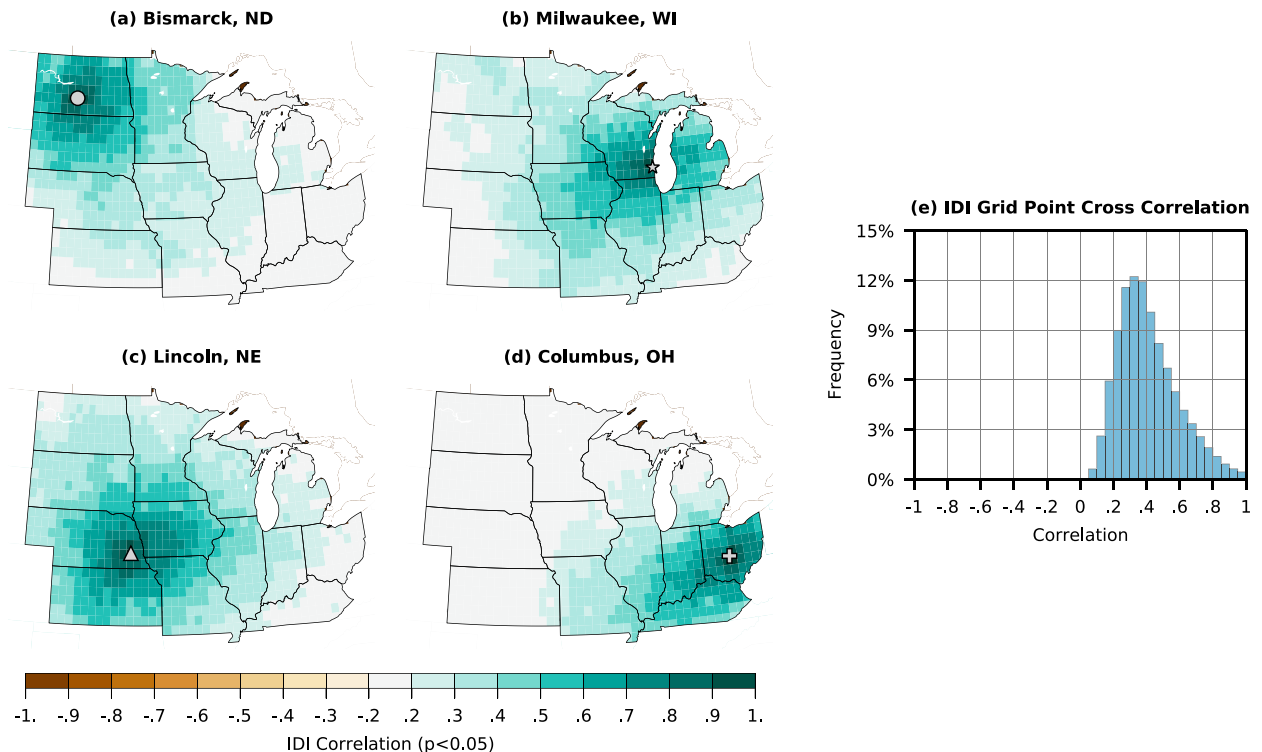


FIG. 2. (a)–(d) Monthly IDI correlation between all grid boxes and the grid box containing each location. (e) Histogram of monthly IDI correlations between any two grid boxes in the domain shown in (a)–(d).

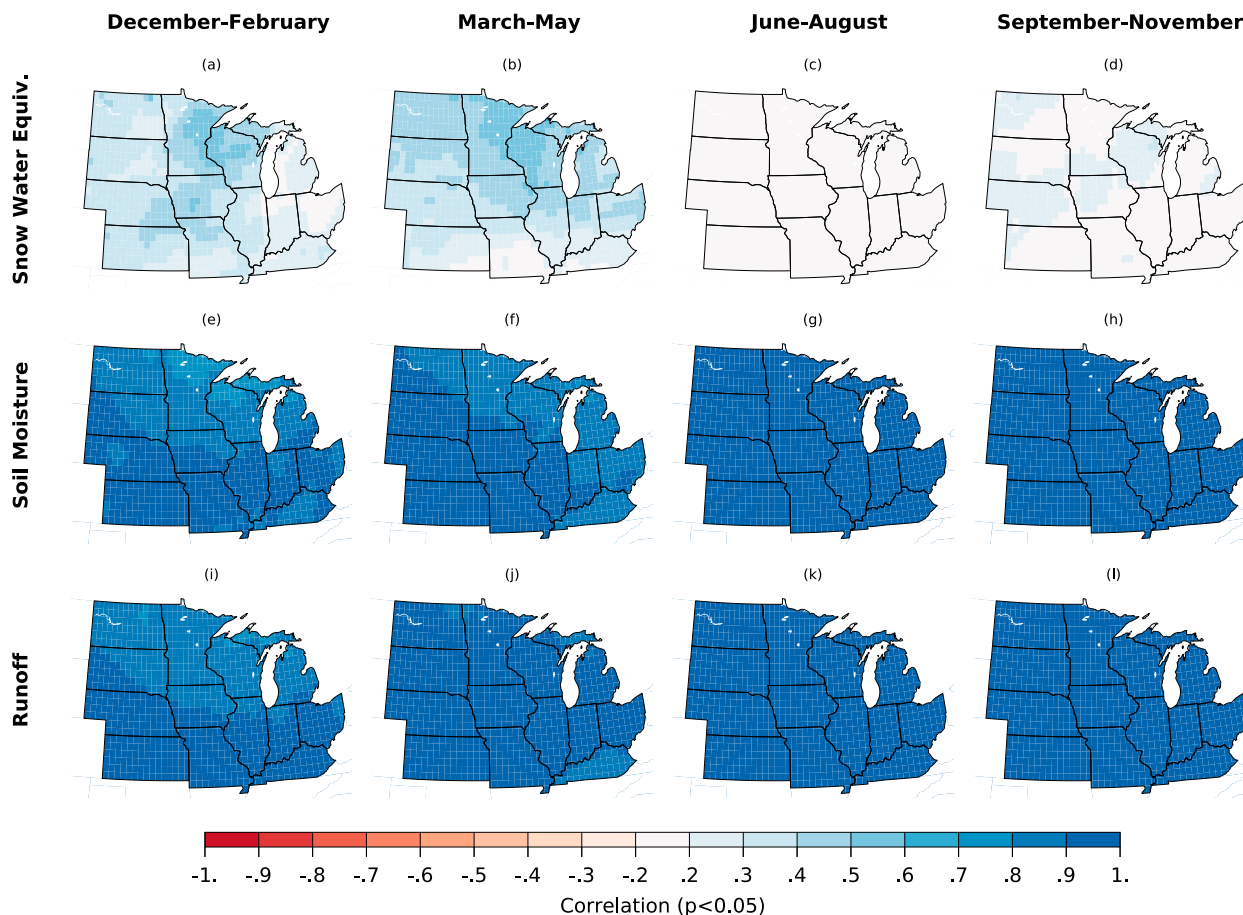


FIG. 3. Correlation of monthly IDI and (a)–(d) snow water equivalent, (e)–(h) soil moisture, and (i)–(l) runoff grouped by season. Correlations are significant at  $p < 0.05$ .

four coherent areas of hydroclimatic variability identified using a hierarchical clustering algorithm applied to the monthly IDI for all grid boxes. We employ Ward's method (Ward 1963), which reduces the sum of the squared distance between a cluster and each grid box in the Midwest. We select four clusters to balance our desire to generalize drought behaviors in the Midwest and to identify regions that are representative of the IDI variability of component grid boxes. The IDI for each region is quantified by calculating the average IDI of all grid boxes within them. We apply the perspective of Mo (2011) to identify drought events based on the regional IDI, whereby a drought event is defined as the time from which IDI falls below  $-0.8$  standardized departures (onset) to when the IDI exceeds  $-0.2$  standardized departures (demise), which ensures complete recovery. IDI variability for each of the identified four regions are related to SST and 300-hPa meridional wind anomalies during 1916–2015 to better establish a predictive understanding of regional hydroclimatic drivers in the Midwest. Monthly SST anomalies are from the Extended Reconstructed SST version 5 dataset (Huang et al. 2017), and monthly 300 hPa meridional wind anomalies are from the Twentieth Century Reanalysis version 3 (Slivinski et al. 2019).

We end our analysis in 2015 because it is the final year of the Twentieth Century Reanalysis version 3.

### 3. Results

#### a. Local hydroclimatic variability

To establish a baseline from which to probe drought characteristics across the Midwest, we begin with an analysis of spatiotemporal precipitation variability at the gridbox scale. A strong gradient in calendar year average precipitation is observed along a west to east oriented axis extending from the Northern Great Plains to the Ohio River Valley (Fig. 1b). The location of the strongest change in annual average precipitation falls between the 95th and 100th west meridians, considered the dividing line between the humid eastern and the semiarid western United States (Seager et al. 2018). Areas in Ohio, Indiana, Illinois, and Missouri on average receive in excess of 1000 mm of precipitation each calendar year while areas in the Dakotas, Nebraska, and Kansas receive between 500 and 700 mm.

Calendar year average precipitation totals are related to differences in the precipitation seasonal cycle across the Midwest (boxplots in Fig. 1). Areas with a shorter wet season/longer dry season observe less annual average rainfall than areas

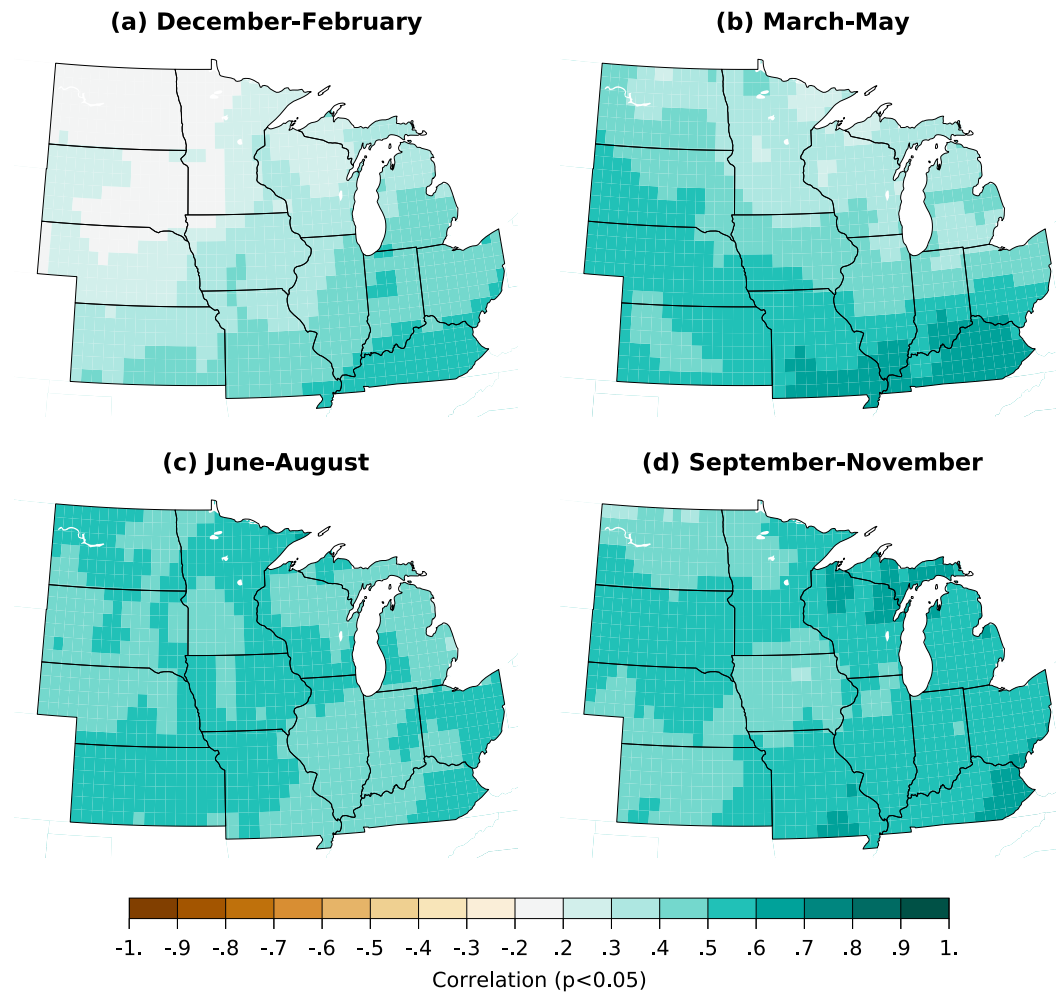


FIG. 4. Correlation of monthly IDI change and precipitation anomaly grouped by season. Correlations are significant at  $p < 0.05$ .

that experience rainfall that is more evenly distributed across the calendar year. The western and northwestern areas of the Midwest, as represented by Bismarck, North Dakota, experience a single wet season spanning May–September, reaching a maximum in June. Also, the variability of precipitation, measured by the interquartile range and extremes relative to the median, are largest in March–May and September–November and smallest during the height of the wet season. A transition to less pronounced and shorter dry seasons occurs as one moves south and east in the Midwest. Lincoln, Nebraska, has a dry season during December–February, but receives appreciable rainfall on average during the other nine months, with a peak spanning late spring to early fall. Columbus, Ohio, representing southeastern areas of the Midwest United States, does not have pronounced wet and dry seasons. Even though the largest monthly precipitation totals in Columbus occur on average in spring and summer, appreciable precipitation is still observed in fall and winter.

Motivated by changes in the precipitation annual cycle across the Midwest, we assess the spatial scales of drought

variability in the region by examining monthly IDI correlations between grid boxes (Fig. 2). In line with Oladipo (1986), we find that drought variations among most grid boxes in the region are not closely related, which affirms that drought in the Midwest generally occurs at local-to-regional spatial scales. Examples of the spatial drought patterns related to the IDI for four grid boxes are presented in Figs. 2a–d. The correlations show that drought is related to a small area surrounding each grid box, and that drought variability can be dissimilar even for locations that share similar hydroclimates (i.e., Milwaukee, Wisconsin, and Columbus, Ohio). More generally, a histogram of monthly IDI cross correlations among all grid boxes in the Midwest (Fig. 2d) further reinforces that the coherence of drought variations in the Midwest is generally marginal. The most likely cross correlation is about 0.3 and just 25% of the grid boxes are correlated at 0.6 or greater.

Based on the complexity of local precipitation and IDI variations across the Midwest, we apply a more nuanced approach to investigating drought than simply relying on area averages of the IDI over the entire region. Our approach

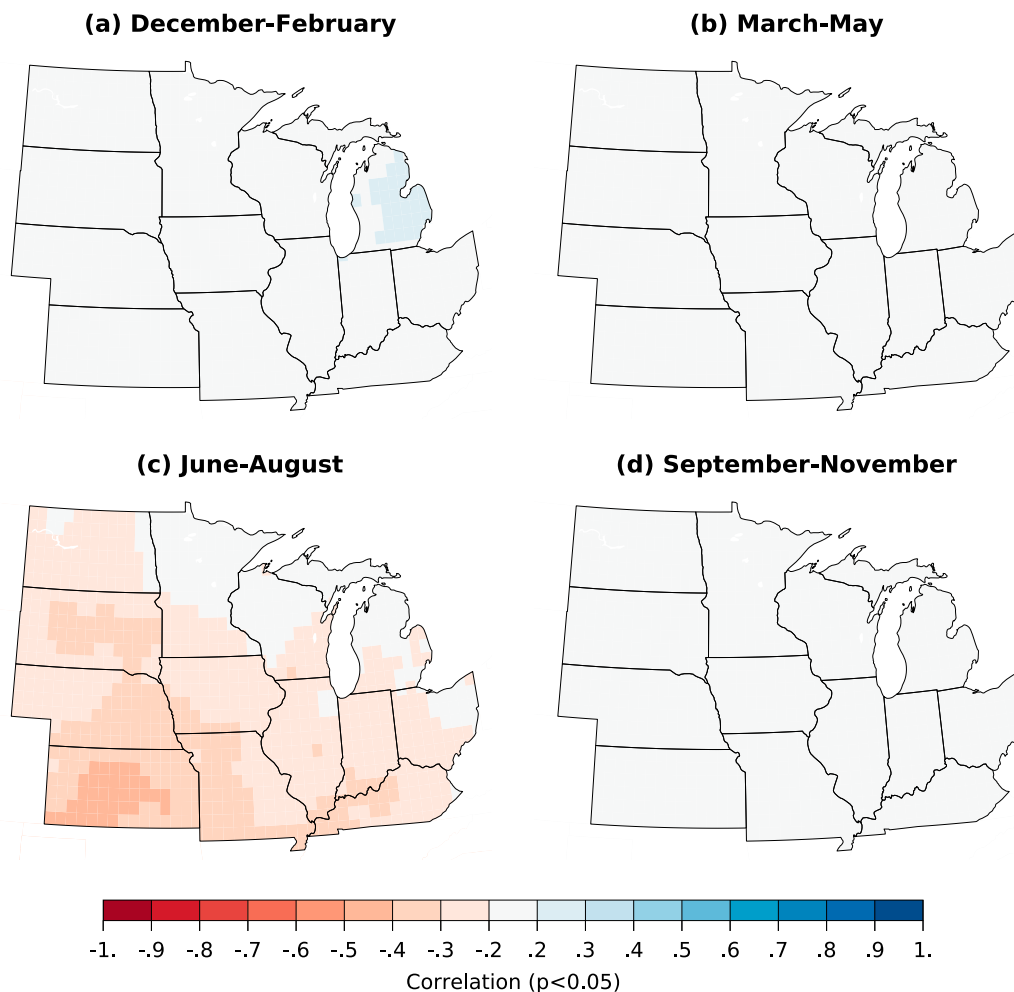


FIG. 5. Correlation of monthly IDI change and 2-m temperature anomaly grouped by season. Correlations are significant at  $p < 0.05$ .

includes examining drought drivers at local scales (i.e., each grid box) and examining drought over coherent regions of IDI variability identified from a hierarchical cluster analysis. We examine local drivers of the IDI in the remainder of this section and the characteristics and predictability of drought over the identified subregions in the following section.

We begin our examination of local drought drivers in the Midwest by investigating the contribution of the IDI's component variables—soil moisture, snow water equivalent, and 3-month runoff—to its variability during 3-month seasons (Fig. 3). The contributions are quantified via correlations calculated from monthly data grouped by 3-month season: December–February, March–May, June–August, and September–November. Soil moisture and runoff overwhelmingly drive the IDI during all seasons; especially in June–August and September–November as their correlations with the IDI exceed 0.9 regionwide. This is expected, since Mo and Lettenmaier (2018) also indicated that total moisture storage, which is entirely due to soil moisture in the warm seasons, and 3-month runoff share the same time scales in the land surface

models used. Snow water equivalent plays a role in driving the IDI during the cold seasons while soil moisture and runoff play slightly less of a role. Statistically significant correlations between snow water equivalent and the IDI are found over most of the region in December–February and March–May in the eastern Plains and Great Lakes region north of 42°N.

We now turn our attention to probing variables related to IDI variability that are forecast on an operational basis, namely, precipitation and 2-m temperature, to provide further insight into our predictive understanding of Midwest drought. We note that other factors like evapotranspiration (e.g., Kim and Rhee 2016), soil type and plant biology (e.g., Xia et al. 2014) play an important role in shaping drought, but we focus here on quantities that are forecast on a regular basis by operational prediction centers like the NOAA Climate Prediction Center.<sup>1</sup> For all seasons, the magnitude of the

<sup>1</sup> <https://www.cpc.ncep.noaa.gov/products/predictions/30day/>.

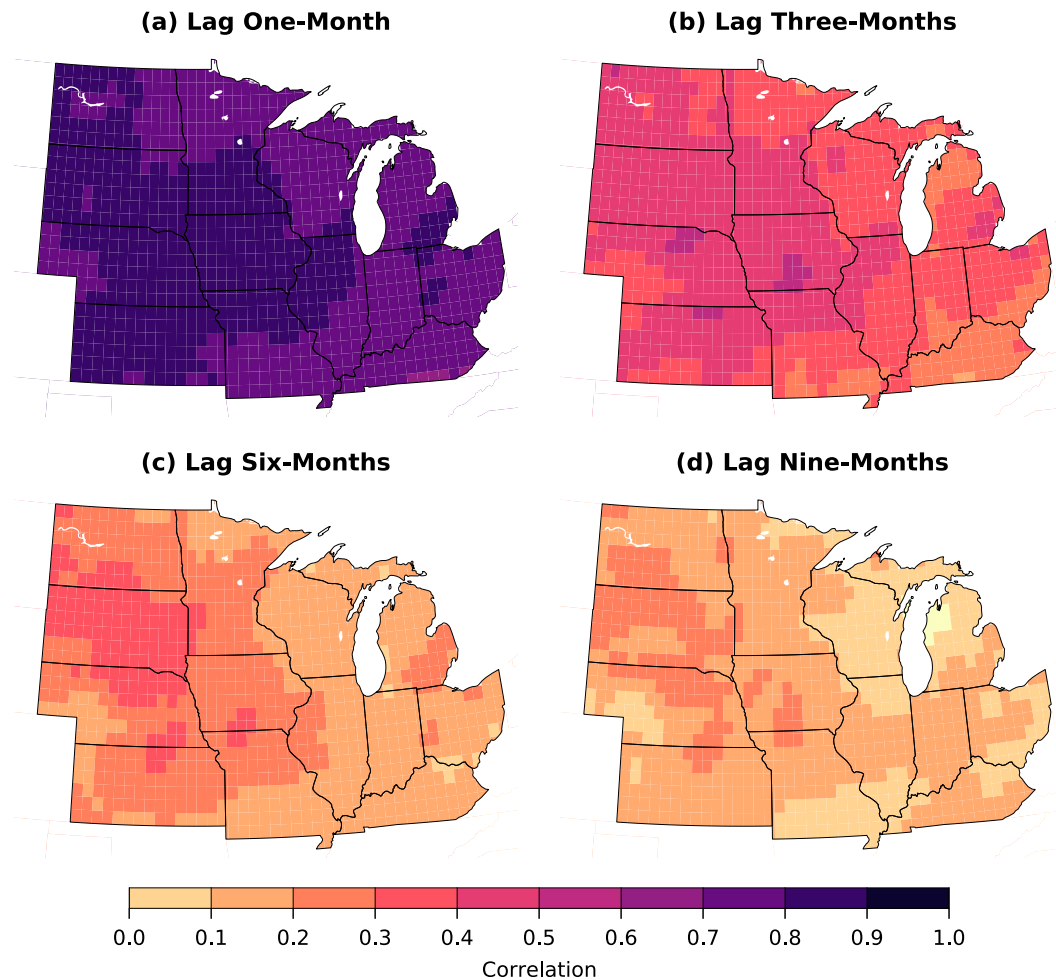


FIG. 6. Serial IDI correlation at (a) 1-, (b) 3-, (c) 6-, and (d) 9-month lags.

correlations between IDI and precipitation (Fig. 4) dwarf those between IDI and temperature (Fig. 5), indicating the primacy of precipitation in driving drought as measured by this IDI in the Midwest. Precipitation and IDI correlations generally exceed 0.5 during all seasons and most areas of the region, while temperature and IDI correlations are only statistically significant in June–August. The contribution of temperature to IDI variations in June–August is especially relevant to rapid drought development, as above average temperatures increase atmospheric evaporative demand and deplete land surface moisture. The only area and season in which this generalization does not hold is in the Northern Plains area of the Midwest in December–February, likely because this is a climatological dry season and a time of year in which the ground can be frozen. Correlations between precipitation and IDI are generally consistent during the warm seasons, though they are slightly lower in the March–May and September–November seasons than in June–August. A possible reason for these interseasonal differences is the lower (higher) precipitation variability relative to the median during the summer (shoulder) season(s) (Fig. 1).

We conclude our analysis of local drought drivers by considering the persistence of the IDI though an examination of

its serial correlation at 1-, 3-, 6-, and 9-month lags (Fig. 6). As expected, an *e*-folding decay in the magnitude of the IDI autocorrelations is apparent throughout the Midwest (e.g., Kumar et al. 2019). Nonetheless, the magnitude of the IDI autocorrelation at a 3-month lag throughout the region is on par with the correlation between IDI and precipitation during most seasons (cf. Figs. 6 and 4), which suggests that the persistence of the IDI generally makes it a good predictor of itself a few months into the future. Also noteworthy is that the magnitude of the autocorrelation at all lags varies spatially, with higher values in the Great Plains compared to areas in the Ohio Valley. This indicates that drought is more persistent in the semiarid regions with a distinct seasonal precipitation cycle than in the more humid climates in which appreciable precipitation is observed during all months of the year.

#### b. Regional drought characteristics and predictability

Given the large spatial variations of hydroclimate in the Midwest (Figs. 1 and 2), a hierarchical cluster analysis based on Ward's method was applied to the monthly IDI in each grid box to identify regions of coherent drought variability (Fig. 7).

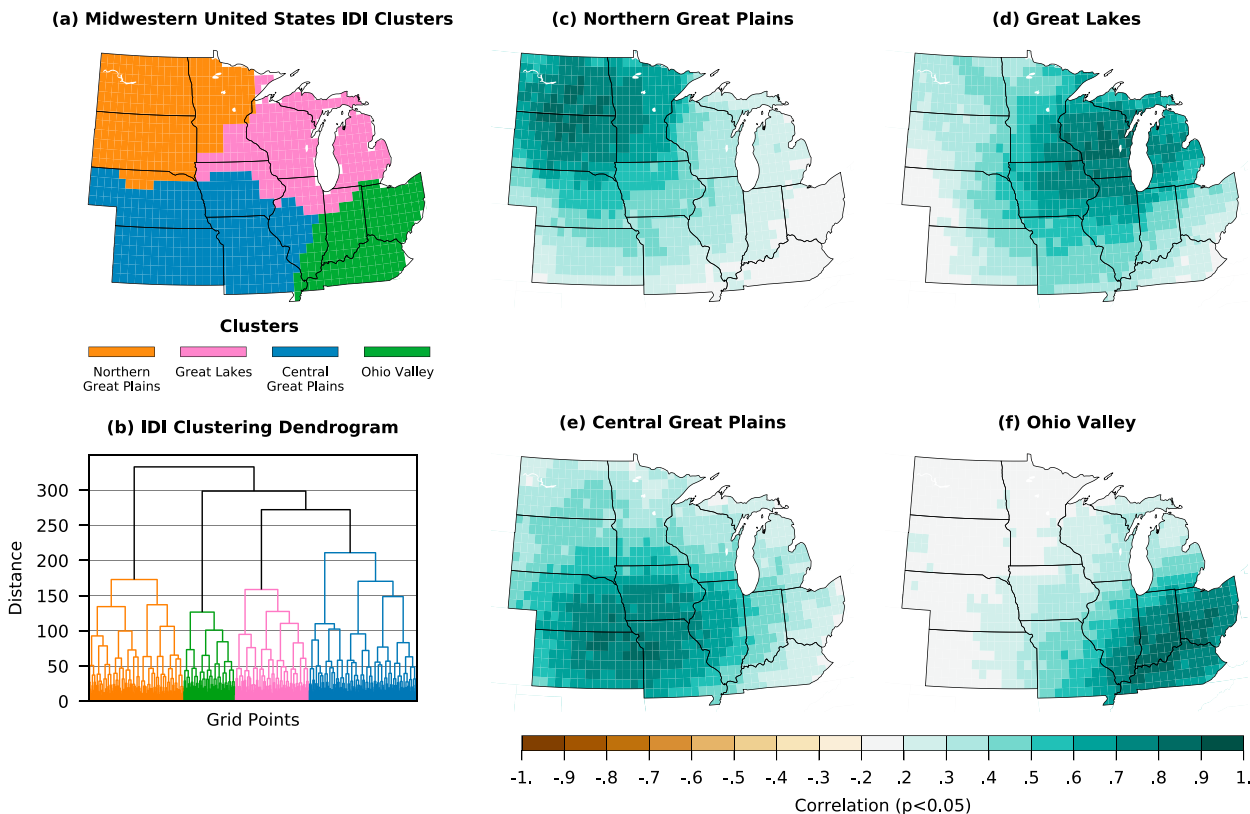


FIG. 7. (a) Four regions identified by applying Ward’s clustering method on monthly IDI during 1916–2015 over the plotted domain. (b) Hierarchical clustering dendrogram associated with (a). Correlation of grid box average IDI over the (c) Northern Great Plains, (d) Great Lakes, (e) Central Great Plains, and (f) Ohio Valley regions and IDI for each grid box.

We select four clusters to balance our desire to generalize drought behaviors in the Midwest and to identify regions that are representative of the IDI variability of component grid boxes. The four identified clusters span approximately the quadrants of the Midwest: the Northern Great Plains in the northwest, the Great Lakes in the northeast, the Central Great Plains in the southwest, and the Ohio Valley in the southeast (Fig. 7a). The clustering dendrogram, indicating which grid boxes belong to each of the four clusters and how they may be further divided into more clusters, is shown in Fig. 7b. Correlations between the average IDI of all grid boxes within the clusters and each grid box indicate that the four regions generally represent the IDI variability within them (Figs. 7c–f). Greater than three quarters of the grid points in each region are correlated with the region average at more than 0.7.

Figure 8, time series of the average IDI of all grid boxes in each of the four regions during 1916–2015, illustrates intricacies of regional drought within the Midwest and highlights considerable hydroclimatic differences between each region. Though annual droughts are a feature in all four regions, the variability of IDI, persistence of low IDI, the clustering of low and high IDI episodes in the same decade, and multidecadal IDI variability are largely different. Nonetheless, there are seven epochs in which all four regions experienced low IDI

simultaneously, and these epochs correspond to a subset of the 16 “Great Droughts” identified by Mo and Lettenmaier (2018). These epochs include 1917/18, 1925, 1933/34, 1939/40, 1963/64, 1988, and 2012/13.

Salient features of IDI variability in each of the four regions are as follows. Note that the 12-month running average IDI is shown in Fig. 8 to further highlight key aspects of drought variability and that 12-month running average IDI based in each of the land surface models is also shown to demonstrate potential uncertainties. The intermodel differences are not large, but notable enough in some epochs to appreciate the uncertainty as a potential limitation of the study. In the Northern Great Plains (Fig. 8a), aside from semiregular annual hydroclimatic variability between 1940 and 1970, the Dust Bowl spanning 1934–41 and the wet epochs of the 1980s, 1990s, and early 2010s stand out as the most prominent features in the IDI time series. Other noteworthy droughts in the Northern Great Plains included 1958–63, 1977, the late 1980s, and 2012.

Despite its proximity to the Northern Great Plains, the Great Lakes experienced rather different hydroclimatic variability during 1916–2015 (Fig. 8b), further highlighting the value of separating the Midwest into smaller regions for the purpose of studying drought. Not only was the timing of positive and negative regional IDI values different between

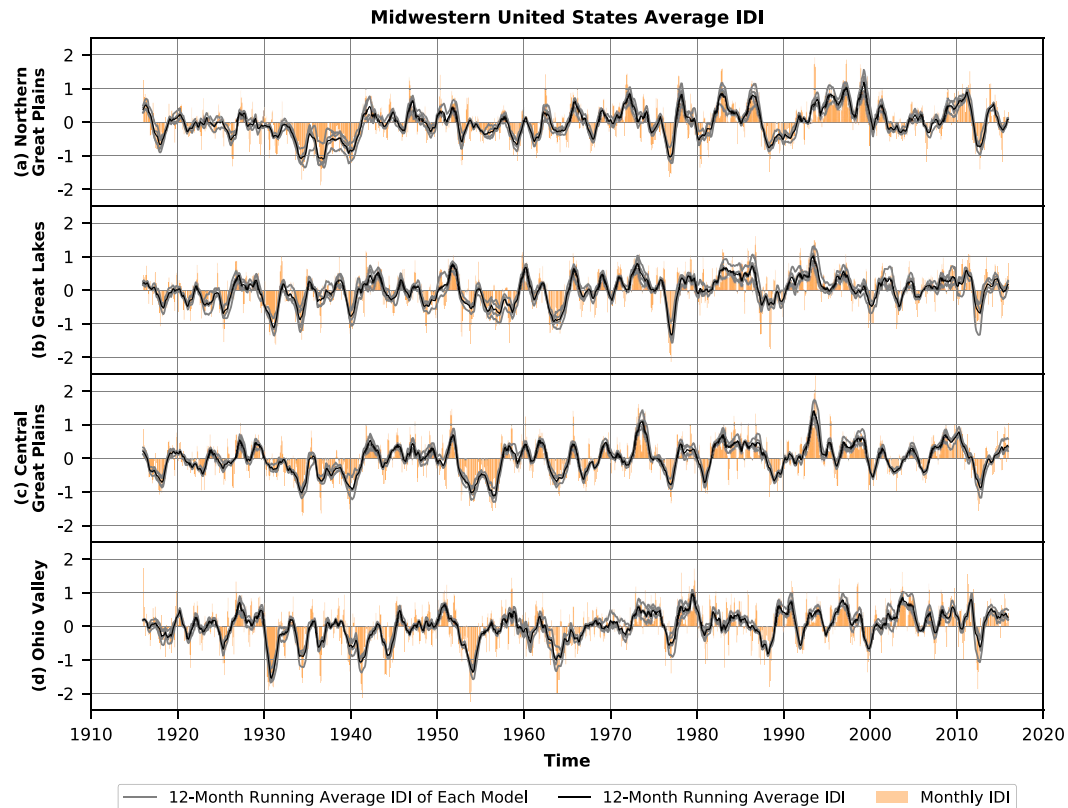


FIG. 8. Time series of gridbox average IDI in standardized departures over the (a) Northern Great Plains, (b) Great Lakes, (c) Central Plains, and (d) Ohio Valley regions of the midwestern United States. Shown is the monthly IDI (orange bars), the 12-month running average IDI (black line), and the 12-month running average IDI constructed from each of the four land surface models to demonstrate uncertainty among them.

the Northern Great Plains and the Great Lakes, the persistence of such values differed as well. The Great Lakes did not experience the Dust Bowl with such vigor; in fact, drought was only felt in 1931 and 1933. The epoch in which drought was most prevalent spanned the mid and late 1950s, and even during that time there were indications of brief drought relief as IDI approached and even exceeded zero. Other noteworthy droughts in the Great Lakes region occurred in the mid-1960s and 1977.

Regional average IDI variability over the Central Great Plains (Fig. 8c) shares considerable commonality with the Northern Great Plains, owing to their geographical location, and similarities in their hydroclimates as indicated by the precipitation annual cycle (Fig. 1) and the serial autocorrelation of IDI (Fig. 6). The Dust Bowl stands out prominently in the IDI time series spanning the 1930s and early 1940s. This region also experienced a significant prolonged drought spanning 1952–57. Though single-year droughts have occurred since 1980 (e.g., 1981, 1988, 2000, 2012), the IDI was predominantly above average, and considerably so, after 1980.

Ohio Valley hydroclimate had the least in common with the other regions in the Midwest during 1916–2015 (Fig. 8d). Not only was the timing of above and below average IDI different from the other regions, the variability of the IDI was considerably larger than each of the other regions as well. The 1930s

and early 1940s were generally a dry time in the Ohio Valley, as indicated by annual droughts in 1931, 1934, and 1941; however, between those droughts above average IDI conditions occurred, which sets this region apart from each of the others. Like the Central Great Plains and Great Lakes, the mid-1950s and mid 1960s were also a dry time in the region. Since 1970, there have been a few single-year droughts, namely, 1977, 1988, 2000, and 2012, but otherwise a wetter climate relative to the past prevailed, as the 1970s, 1990s and 2000s saw persistently high IDI values.

We now probe the characteristics of regional droughts in the Midwest during 1916–2015 based on a collection of events identified using the method of Mo (2011), whereby droughts begin when the regional average IDI falls below  $-0.8$  and persist until the regional average exceeds  $-0.2$ . Figure 9, the frequency of drought persistence in each of the four Midwest regions, illustrates that the likelihood of drought duration depends on location. Droughts last considerably longer in the Great Plains than they do in the Great Lakes or Ohio Valley. The likelihood of drought lasting for at least one month in each region based on the drought definition we adopted is approximately 20%–22%, which is generally consistent with the drought definition used by the U.S. Drought Monitor (Svoboda et al. 2002). An  $e$ -fold decay in the frequency of drought as a function of persistence is noted for each region, though the

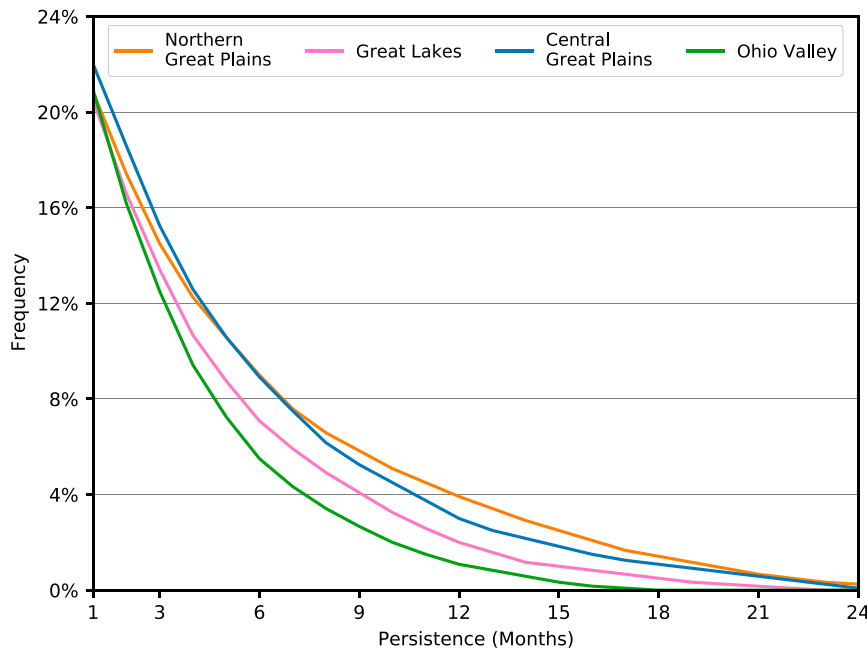


FIG. 9. Cumulative histogram of drought persistence.

magnitude of the decay varies from one region to the next. For example, the Northern Great Plains was 4 times more likely to experience a drought lasting at least 12 months than the Ohio Valley. This is consistent with the larger magnitude serial correlation of the local IDI shown in Fig. 6, which is linked to the climatological precipitation seasonal cycles, in which much of the Northern Great Plains experiences a single wet season while the Ohio Valley receives precipitation during all calendar months (Fig. 1).

The collection of drought events based on our definition indicates preferred seasons of drought onset and demise in each region of the Midwest (Fig. 10). The preferred seasons of onset and demise generally follow the precipitation seasonal cycle, whereby droughts tend to begin and end during wet seasons, and particularly during times in those wet seasons when the precipitation variability relative to the median is either largest or smallest (Fig. 1). For the Northern Great Plains, droughts overwhelmingly begin and end outside of winter, which is on average the dry time of year. Drought onset is most likely to occur in September–November and March–May, the times of year in which the precipitation variability is largest compared to the median, with a dip in the frequency of onset in June–August, the wettest 3-month season with relatively low precipitation variability. Drought demise is most likely to occur during the wetter seasons, and in particular during June–August and September–November. The frequency of drought onset and demise in the Central Great Plains is quite similar to that of the Northern Great Plains. This is not a surprising result given similarities between the two hydroclimates.

Drought onset and demise in the Great Lakes and Ohio Valley regions of the Midwest occur more equitably across the seasons than was observed over the Great Plains regions.

For the Great Lakes region, drought onset and demise occur nearly as frequently in December–February, March–May, June–August, but increase greatly in September–November. The higher frequency of onset and demise in September–November relative to the other seasons can be attributed to the precipitation seasonal cycle, which is quite variable relative to the mean. For the Ohio Valley region, owing to a relatively flat precipitation seasonal cycle, we see little difference in the frequency of drought onset and demise across the seasons. However, there are slight increases in March–May and September–November. March–May is the wettest 3-month season, and there is considerable precipitation variability, while September–November is the driest of the 3-month seasons, which too experiences considerable precipitation variability relative to the other seasons.

A key consideration of drought in the Midwest is how quickly they can emerge, an event known as flash or rapid onset droughts (Otkin et al. 2018; Pendergrass et al. 2020), given recent experiences like the 2012 event. Instances of rapid changes in the regional IDI time series from one month to the next are apparent (Fig. 8), and we probe the likelihood of these changes using histograms of monthly changes grouped by season (Fig. 11). Note that flash onset droughts can occur in as little as a few weeks so that monthly IDI changes may not fully capture the speed at which this class of droughts emerges. Indicated hereby is a distinct seasonality and regionality to the speed of IDI changes. September–November and June–August stand out as the seasons in which the largest month-to-month changes in IDI occur, then followed by March–May. Large positive changes during these seasons are related to abundant precipitation that can fall while large negative changes during these seasons are related to the lack of

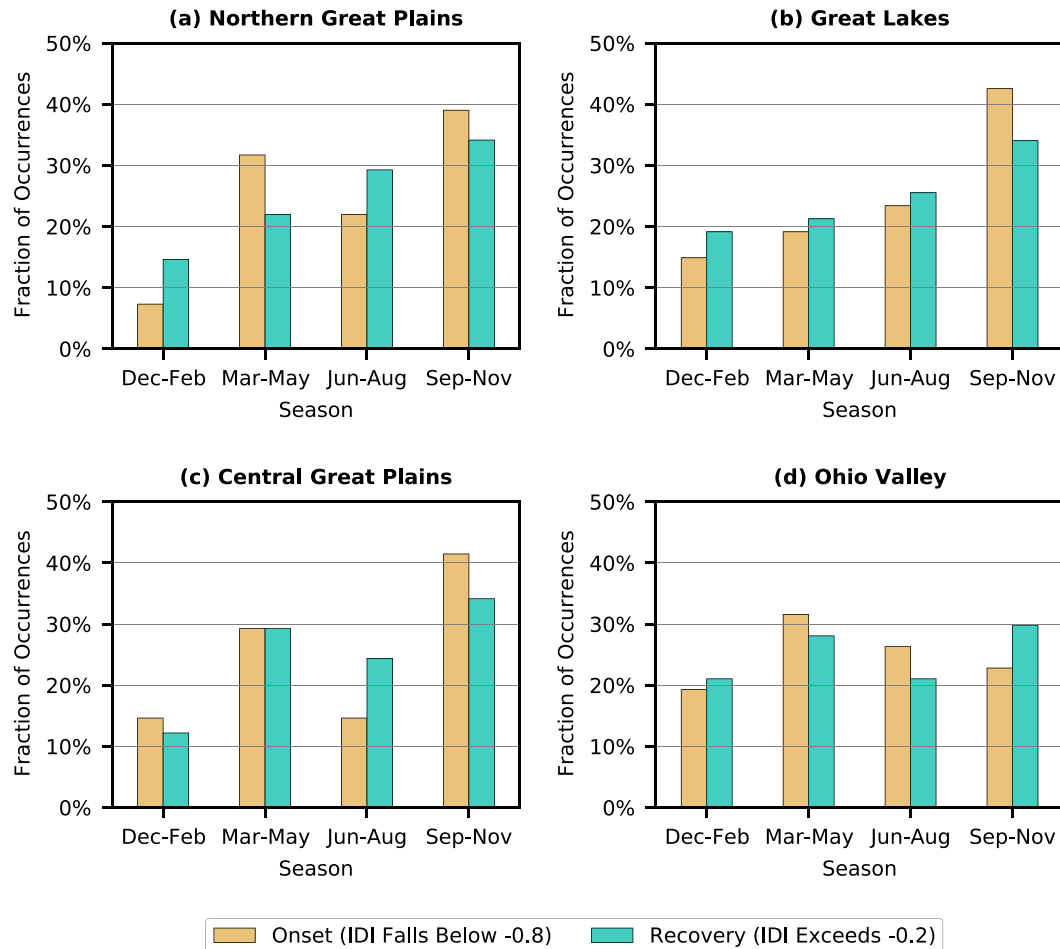


FIG. 10. Fraction of drought onset and recovery in each region by season.

precipitation and considerable evapotranspiration that can occur during warm seasons. The smallest changes in IDI occur in December–February over all regions except the Ohio Valley, likely a result of it being the cold and/or dry season in those three regions. In the Ohio Valley, larger changes in IDI in December–February are possible because appreciable precipitation is still observed this time of year and the ground may not be frozen throughout.

Toward establishing a predictive understanding of the causes of Midwest hydroclimatic variability, we relate monthly changes in regional average IDI to SST and 300-hPa meridional wind anomalies. Relationships with meridional wind anomalies help to diagnose how the atmospheric circulation shapes drought, while SST anomalies, especially those over the Pacific Ocean, may serve as a key source of longer-lead predictability for drought because of their slow variations and established effects on global climate (e.g., Dai and Wigley 2000; Kiladis and Diaz 1989). Since a key mode of Pacific SST variability, El Niño–Southern Oscillation, is related to temperature and precipitation over the United States (e.g., Ropelewski and Halpert 1986; Kellner and Niyogi 2015), it is expected to play a role in changes in drought variability in at least some regions of the Midwest.

Regressions of monthly changes in IDI onto SST anomalies grouped by 3-month seasons yield few relationships between regional drought and coherent SST patterns representing predictable modes of climate variability (Fig. 12). Only the Ohio Valley is significantly related to SST patterns (Deser et al. 2010; Messié and Chavez 2011) associated with ENSO. This is apparent in December–February (Fig. 12a), given the negative regressions over the tropical central Pacific Ocean, and less so in June–August (Fig. 12c), as indicated by some semblance of SSTs related to ENSO in the subtropical and extratropical North Pacific Ocean. This wintertime relationship makes sense because precipitation in the Ohio Valley, where appreciable precipitation is measured during this season, is generally below average during El Niño events and above average during La Niña events (Kellner and Niyogi 2015). Otherwise, no significant relationships are found between IDI over the Northern Great Plains (Fig. 12, bottom row), Central Great Plains, and Great Lakes regions (not shown for brevity), and SST related to coherent or predictable modes of climate variability. The results suggest that the lead-dependent predictability of drought over these regions and seasons is limited since slow-varying predictors in the climate system (e.g., SSTs) do not apply.

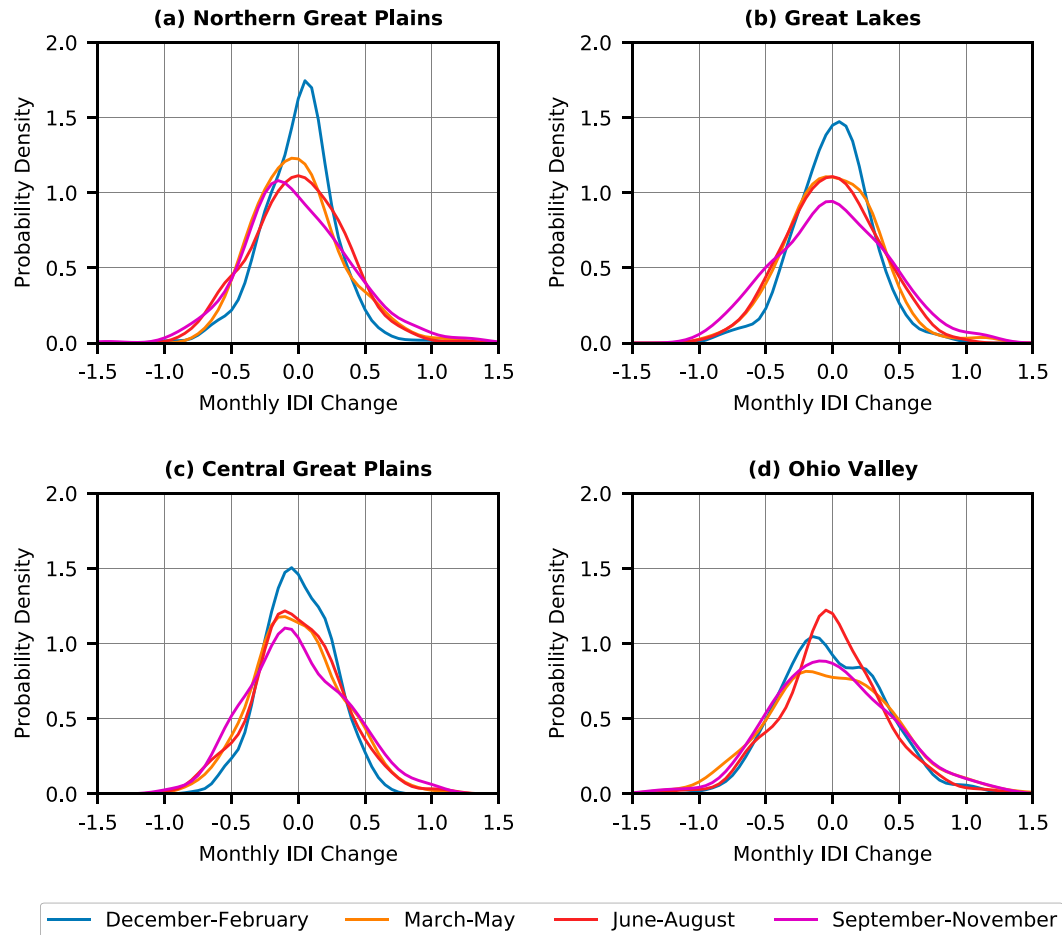


FIG. 11. Histograms smoothed by a kernel density estimator of monthly IDI change in standardized departures grouped by season.

Regressions of monthly IDI changes on to 300-hPa meridional wind anomalies grouped by 3-month season (Fig. 13) indicate that regional droughts are related to clearly defined wave trains, or alternating areas of anomalous northerly and southerly winds, across the Northern Hemisphere. Except for the Ohio Valley in December–February, the wave trains for the combination of regions and seasons are not related to SSTs (cf. Figs. 12a and 13a), and are therefore linked to variability internal to the atmosphere. For the Ohio Valley in December–February (Fig. 13a), the circulation pattern closely resembles that commonly associated with ENSO (e.g., Horel and Wallace 1981; Rasmusson and Wallace 1983), with a wave train emanating from the western tropical Pacific and arcing over North America. By contrast, the wave trains related to Northern Great Plains (Fig. 13, bottom row), Central Great Plains, and Great Lakes regions (not shown for brevity) are clearly defined, but are confined to the midlatitudes. This indicates that the wave trains during these seasons are related to variability internal to the atmosphere, similar to the finding of Seager et al. (2020) relevant to the Southern Plains. The results suggest that the wave trains are unlikely to be predictable at lead times longer than a week or two, given the current predictability

limits of the atmospheric wave trains related to drought in initialized forecast systems (DeAngelis et al. 2020).

The abundance of regional droughts in the 1930s and 1950s and the relative scarcity of regional drought after the 1990s (Fig. 8) motivate us to probe decadal drought occurrence across the Midwest, as measured by the fraction of time spent below  $-0.8$  IDI during nine nonoverlapping 10-yr periods spanning the twentieth and twenty-first centuries (Fig. 14). Indicated hereby are notable decadal variations in drought prevalence over the Midwest, and that the drought-prevalent decades generally occurred early in our period of record, in line with Mishra and Cherkauer (2010). Drought was especially prevalent in the 1930s and 1950s, as large portions of the Midwest experienced an IDI less than  $-0.8$ , approximately 2–4 times as often as during the 1990s and 2000s.

Significant increases in annual precipitation from 1920–79 to 1980–2009 (Fig. 14; see also Ford 2014; Pryor et al. 2009) explain the observed decrease in drought prevalence in the Midwest during the late twentieth and early twenty-first centuries (Figs. 8 and 14). Comparing a recent 30-yr period to a prior 60-yr period is a common technique for identifying differences within precipitation time series (e.g., Peterson et al. 2013;

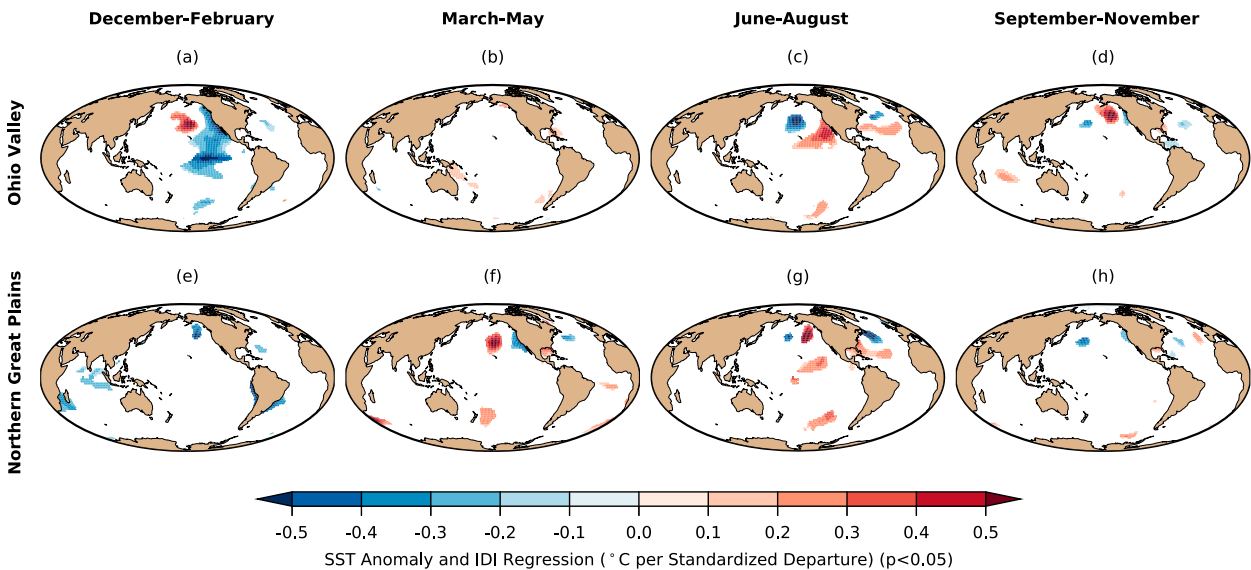


FIG. 12. Regression of monthly average IDI over the (a)–(d) Ohio Valley and (e)–(h) Northern Great Plains regions and SSTs grouped by season. Shading indicates regressions significant at  $p < 0.05$ .

Easterling et al. 2017). Widespread statistically significant increases in annual precipitation were observed over more than 80% of the region (Fig. 15). Increases in annual precipitation of up to 15% occurred over the climatologically driest areas of the Midwest, notably the Great Plains and the Upper Midwest. The climatologically wetter areas in the lower Midwest, Ohio Valley, and Great Lakes regions have experienced more modest annual precipitation increases of up to 9% in the recent 30-yr period compared to the prior 60 years.

#### 4. Summary and conclusions

We examined characteristics and predictability of Midwest drought at local and regional scales using a monthly integrated drought index (IDI) derived from four land surface models forced by observed analyses during 1916–2015. This IDI, constructed using soil moisture, runoff, and snow water equivalent,

was employed so that many facets of drought important to the Midwest may be considered: agricultural, hydrological, and snow. At local scales, we found large spatial variations of hydroclimate, which inspired us to apply a hierarchical cluster analysis to the IDI to identify regions of coherent drought variability. We investigated characteristics of drought over four regions—the Northern Great Plains, Great Lakes, Central Great Plains, and Ohio Valley—and found that the duration of droughts, when they began and ended, and how they varied in time differed between the regions. Likewise, we investigated the predictability of drought over the four regions by relating the regionally averaged IDI to SSTs and aspects of the large-scale atmospheric circulation to determine features of the climate system that may be used to anticipate drought.

The spatial scales of hydroclimatic variability are small compared to the size of the Midwest, which indicates that drought should be examined locally or by individual regions in

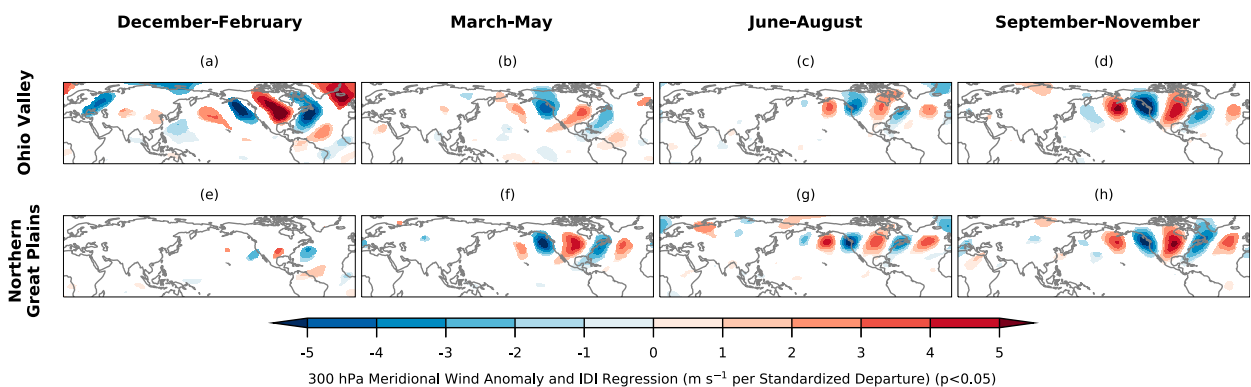


FIG. 13. Regression of monthly average IDI over the (a)–(d) Ohio Valley and (e)–(h) Northern Great Plains regions and 300-hPa meridional wind grouped by season. Shading indicates regressions significant at  $p < 0.05$ .

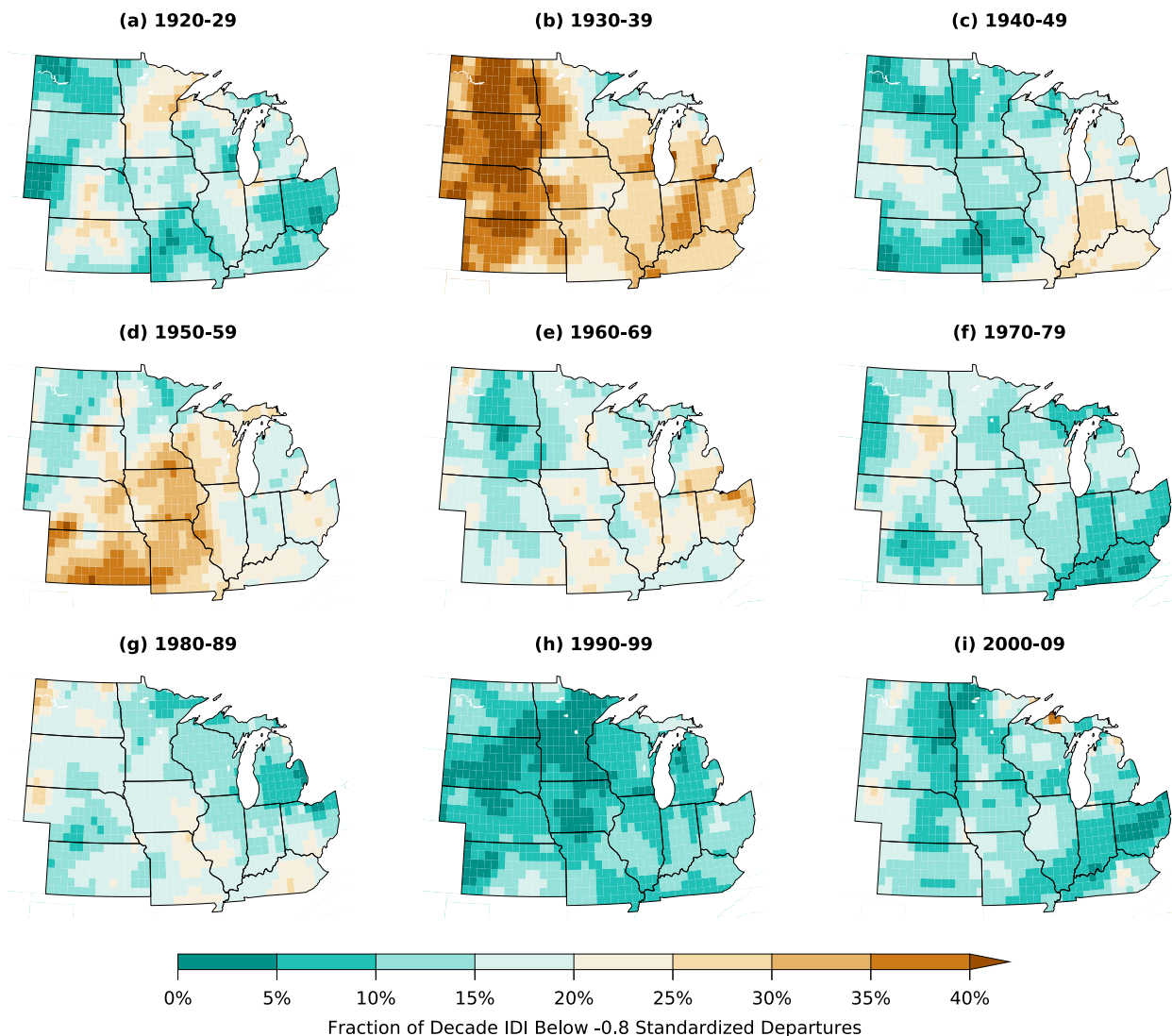


FIG. 14. Fraction of each decade that monthly IDI was below  $-0.8$  standardized departures.

which hydroclimatic variations are coherent. This conclusion was based on the monthly correlations between the IDI in four grid boxes and IDI in all other grid boxes in the Midwest (Fig. 2). We found that the IDI is related to a small area surrounding each grid box, and that drought variability can be dissimilar even for locations that are in relatively close proximity.

Focusing locally, we conclude that of the three variables examined, soil moisture and runoff overwhelmingly drive drought during all seasons based on the IDI we employed (Fig. 3). Correlations between the IDI and soil moisture and runoff exceed 0.8 during all seasons regionwide, and 0.9 during the warm seasons. Snow water equivalent plays a secondary role during the cool seasons of December–February and March–May in the eastern Great Plains and Great Lakes region. Regarding precipitation and temperature, which are forecast by operational prediction centers and are considered in drought outlooks, we conclude that for all seasons the

magnitude of the correlations between IDI and precipitation dwarf those between IDI and temperature, indicating the primacy of precipitation in driving drought as measured by this IDI in the Midwest (cf. Figs. 4 and 5). Significant relationships between temperature and IDI are found only during June–August, but the correlations between the two variables is nonetheless marginal.

Balancing our desire to generalize drought in the Midwest and to identify regions of coherent hydroclimatic variability, we separated the Midwest into four regions based on an objective hierarchical clustering method applied to the IDI (Fig. 7). The four regions we identified include the Northern Great Plains, Great Lakes, Central Great Plains, Ohio Valley. These regions are representative of the area within them, as greater than three quarters of the grid points in each region are correlated with the region average at more than 0.7. We identified differences in the drought characteristics between each of the four regions based on time series of regionally

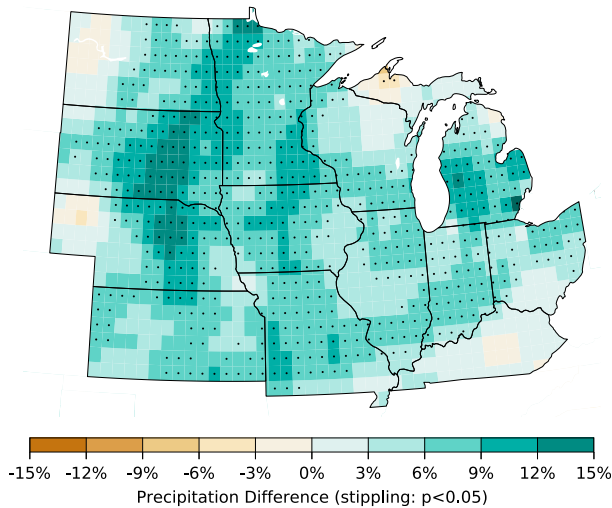


FIG. 15. Calendar year average precipitation difference between 1980–2009 and 1920–79. Stippling indicates differences significant at  $p < 0.05$  based on a bootstrapping approach.

averaged IDI. We found that the variability of IDI, clustering of low and high IDI episodes in the same decades, and multi-decadal IDI variability are largely different between each region (Fig. 8). We further probed the differences in drought characteristics—notably onset, demise, and persistence—between each region based on a collection of events, whereby droughts begin when the regional average IDI falls below  $-0.8$  and persist until the regional average exceeds  $-0.2$ . Droughts last longer in the Great Plains regions than they do in the Great Lakes and Ohio Valley regions (Fig. 9). For example, the Northern Great Plains was 4 times more likely than the Ohio Valley to experience a drought lasting at least 12 months. A distinct seasonality is also noted in drought onset and demise over the Midwest. The precipitation seasonal cycle is the proximate cause of differences in drought length, onset, and demise (Fig. 10). The Great Plains regions experience a single wet season, leading to fewer opportunities for drought amelioration, than the Ohio Valley. The preferred seasons of onset and demise generally follow the precipitation seasonal cycle, both in terms of mean precipitation and variability around the mean. Our analyses of regional drought reaffirm decreases in drought prevalence (Figs. 8 and 14) noted in other studies (e.g., Mo and Lettenmaier 2018). We conclude that the decrease in drought during 1916–2015 are related to statistically significant increases in precipitation throughout the Midwest, with the largest increases observed in the Great Plains.

The relationships between regional IDI and SSTs and 300-hPa meridional winds were diagnosed to establish whether slow-varying behaviors in the climate system could be used to anticipate future droughts. We conclude that only the Ohio Valley is related to slow-varying SSTs consistent with ENSO during December–February (Fig. 12), indicating that longer-lead predictability is limited to only this region and season by virtue of the persistence of ENSO during this time of the year. IDI variations in all other seasons and regions are related to

atmospheric wave trains spanning the Pacific–North American region, highlighting the importance of internal atmospheric variability in shaping Midwest drought (Fig. 13).

## 5. Discussion

The overarching objective of our study was to further establish a predictive understanding of drought in the Midwest at spatial scales useful to drought early warning efforts. We set out to identify drought behaviors in coherent regions of hydroclimatic variability that may be used to anticipate future droughts, including their key characteristics and relationships with behaviors elsewhere in the Earth system that may be used as drought predictors. Our study uses outputs from four land surface models to quantify drought. While the land surface models are constrained by estimates of observed conditions during 1916–2015, it must be noted that a limitation of our study is that none simulate the land surface perfectly. Nonetheless, the use of four models should mute biases introduced by a single model and it does not appear that each of the models are systematically different since they in large part capture the same regional drought variability (Fig. 8).

Accurate drought predictions are notoriously difficult, especially with regard to drought development (see NOAA Climate Prediction Center’s forecast skill<sup>2</sup>). ENSO is a primary predictor of regional climates across the globe, so we focused on its explanatory power of IDI variability in the Midwest regions we identified. We found just one region and season in which ENSO plays a key role, that being the region containing the Ohio Valley during winter. We did, however, find that atmospheric wave trains are related to regional hydroclimates in the Midwest, which indicates some systematic cause of drought. The current predictability limits of the atmospheric wave trains related to drought in initialized forecast systems is approximately two weeks (DeAngelis et al. 2020), which poses a challenge for subseasonal to seasonal forecasting. However, recent studies have highlighted Midwest drought prediction skill stemming from other large-scale teleconnections, such as that from the Pacific–North American pattern (PNA) and soil moisture initial states (DeAngelis et al. 2020; Shin et al. 2020; Zhuang et al. 2021), which should serve as a source of optimism.

A noteworthy feature of regional hydroclimates within the Midwest is the decreasing prevalence of drought during our period of record. The decreasing drought prevalence is related to a wetter epoch in 1980–2009 relative to 1920–79. It must be noted that this is not a formal attribution of a secular trend to a wetter climate as a result of anthropogenic influences. Decadal drought variations have been shown to be a natural component of the climate system in the Midwest, and specifically the Great Plains (e.g., Schubert et al. 2004), so while the timing of dry and wet epochs at the beginning and end of our period of record may be suggestive of a trend toward wetter conditions, this may be due to variability as a result of the natural phasing of wet and dry

<sup>2</sup> [https://www.cpc.ncep.noaa.gov/products/expert\\_assessment/sdo\\_verification/med-pct-area.png](https://www.cpc.ncep.noaa.gov/products/expert_assessment/sdo_verification/med-pct-area.png).

epochs. Further testing with ensembles of climate model simulations from which the contributions of natural decadal variations and anthropogenic influences would need to be used to parse this out.

The observed wetting trend over the Midwest, though reducing the frequency of droughts, has presented the region with other challenges. These challenges include an increase in the frequency of abrupt transitions between flooding and drought, as evidenced by record flooding in 2011, followed by a billion-dollar drought disaster in 2012, which was followed by wetness in 2013 (Ford et al. 2021). Further study on the predictability, variability, and long-term changes in drought and the transition from drought to flooding are essential for a region vulnerable to hydroclimatic extremes.

*Acknowledgments.* The authors thank Dennis Lettenmaier and two anonymous reviewers for detailed and insightful comments that helped us improve the manuscript. The authors also thank Ryan Currier of the NOAA Physical Sciences Laboratory for providing constructive comments that improved an earlier version of the manuscript. The authors gratefully acknowledge Mu Xiao of the UCLA Land-Surface Hydrology Group for arranging access to the VIC, Noah, SAC-SMA, and Catchment land surface model simulations. This work was supported by the National Integrated Drought Information System, the NOAA Climate Program Office Modeling, Analysis Predictions, and Projections Program, and the NOAA Physical Sciences Laboratory.

#### REFERENCES

- Barlow, M., S. Nigam, and E. H. Berbery, 2001: ENSO, Pacific decadal variability, and U.S. summertime precipitation, drought, and stream flow. *J. Climate*, **14**, 2105–2128, [https://doi.org/10.1175/1520-0442\(2001\)014<2105:EPDVAV>2.0.CO;2](https://doi.org/10.1175/1520-0442(2001)014<2105:EPDVAV>2.0.CO;2).
- Bohn, T. J., B. Livneh, J. W. Oyster, S. W. Running, B. Nijssen, and D. P. Lettenmaier, 2013: Global evaluation of MTCLIM and related algorithms for forcing of ecological and hydrological models. *Agric. For. Meteorol.*, **176**, 38–49, <https://doi.org/10.1016/j.agrformet.2013.03.003>.
- Burnash, R. J. C., R. L. Ferral, and R. A. McGuire, 1973: A generalized streamflow simulation system: Conceptual modeling for digital computers. Joint Federal and State River Forecast Center, U.S. National Weather Service, and California Department of Water Resources Tech. Rep., 204 pp.
- Centers for Disease Control and Prevention, 2020: Health implications of drought. <https://www.cdc.gov/ncchd/drought/implications.htm>.
- Chen, P., and M. Newman, 1998: Rossby wave propagation and the rapid development of upper-level anomalous anticyclones during the 1988 U.S. drought. *J. Climate*, **11**, 2491–2504, [https://doi.org/10.1175/1520-0442\(1998\)011<2491:RWPATR>2.0.CO;2](https://doi.org/10.1175/1520-0442(1998)011<2491:RWPATR>2.0.CO;2).
- Dai, A., and T. M. L. Wigley, 2000: Global patterns of ENSO-induced precipitation. *Geophys. Res. Lett.*, **27**, 1283–1286, <https://doi.org/10.1029/1999GL011140>.
- DeAngelis, A. M., H. Wang, R. D. Koster, S. D. Schubert, Y. Chang, and J. Marshak, 2020: Prediction skill of the 2012 U.S. Great Plains flash drought in Subseasonal Experiment (SubX) models. *J. Climate*, **33**, 6229–6253, <https://doi.org/10.1175/JCLI-D-19-0863.1>.
- Deser, C., M. A. Alexander, S.-P. Xie, and A. S. Phillips, 2010: Sea surface temperature variability: Patterns and mechanisms. *Annu. Rev. Mar. Sci.*, **2**, 115–143, <https://doi.org/10.1146/annurev-marine-120408-151453>.
- Diaz, H. F., 1983: Drought in the United States. *J. Appl. Meteor. Climatol.*, **22**, 3–16, [https://doi.org/10.1175/1520-0450\(1983\)022<0003:DITUS>2.0.CO;2](https://doi.org/10.1175/1520-0450(1983)022<0003:DITUS>2.0.CO;2).
- Ducharne, A., R. D. Koster, M. J. Suarez, M. Stieglitz, and P. Kumar, 2000: A catchment-based approach to modeling land surface processes in a general circulation model: 2. Parameter estimation and model demonstration. *J. Geophys. Res.*, **105**, 24 823–24 838, <https://doi.org/10.1029/2000JD900328>.
- Easterling, D. R., and Coauthors, 2017: Precipitation change in the United States. *Climate Science Special Report: Fourth National Climate Assessment, Volume I*, D. J. Wuebbles et al., Eds., U.S. Global Change Research Program, 207–230, <https://doi.org/10.7930/J0H993CC>.
- Eeswaran, R., A. P. Nejadhashemi, F. C. Alves, and B. Saravi, 2021: Evaluating the applicability of soil moisture-based metrics for gauging the resiliency of rainfed agricultural systems in the midwestern United States. *Soil Tillage Res.*, **205**, 104818, <https://doi.org/10.1016/j.still.2020.104818>.
- Ek, M. B., and Coauthors, 2003: Implementation of Noah land surface model advances in the National Centers for Environmental Prediction operational mesoscale Eta model. *J. Geophys. Res.*, **108**, 8851, <https://doi.org/10.1029/2002JD003296>.
- Englehart, P. J., and A. V. Douglas, 2003: Assessing warm season drought episodes in the central United States. *J. Climate*, **16**, 1831–1842, [https://doi.org/10.1175/1520-0442\(2003\)016<1831:AWSDEI>2.0.CO;2](https://doi.org/10.1175/1520-0442(2003)016<1831:AWSDEI>2.0.CO;2).
- Ford, T. W., 2014: Precipitation anomalies in eastern-central Iowa from 1640–Present. *J. Hydrol.*, **519**, 918–924, <https://doi.org/10.1016/j.jhydrol.2014.08.021>.
- , L. Chen, and J. T. Schoof, 2021: Variability and transitions in precipitation extremes in the midwest United States. *J. Hydrometeorol.*, **22**, 533–545, <https://doi.org/10.1175/JHM-D-20-0216.1>.
- Hoerling, M., and Coauthors, 2014: Causes and predictability of the 2012 Great Plains drought. *Bull. Amer. Meteor. Soc.*, **95**, 269–282, <https://doi.org/10.1175/BAMS-D-13-00055.1>.
- Horel, J. D., and J. M. Wallace, 1981: Planetary-scale atmospheric phenomena associated with the Southern Oscillation. *Mon. Wea. Rev.*, **109**, 813–829, [https://doi.org/10.1175/1520-0493\(1981\)109<0813:PSAPAW>2.0.CO;2](https://doi.org/10.1175/1520-0493(1981)109<0813:PSAPAW>2.0.CO;2).
- Huang, B., and Coauthors, 2017: Extended Reconstructed Sea Surface Temperature, Version 5 (ERSSTv5): Upgrades, validations, and intercomparisons. *J. Climate*, **30**, 8179–8205, <https://doi.org/10.1175/JCLI-D-16-0836.1>.
- Huning, L. S., and A. AghaKouchak, 2020: Global snow drought hot spots and characteristics. *Proc. Natl. Acad. Sci. USA*, **117**, 19 753–19 759, <https://doi.org/10.1073/pnas.1915921117>.
- Kahya, E., and J. A. Dracup, 1993: U.S. streamflow patterns in relation to the El Niño/Southern Oscillation. *Water Resour. Res.*, **29**, 2491–2503, <https://doi.org/10.1029/93WR00744>.
- Kalnay, E., and Coauthors, 1996: The NCEP/NCAR 40-Year Reanalysis Project. *Bull. Amer. Meteor. Soc.*, **77**, 437–471, [https://doi.org/10.1175/1520-0477\(1996\)077<0437:TNYRP>2.0.CO;2](https://doi.org/10.1175/1520-0477(1996)077<0437:TNYRP>2.0.CO;2).
- Kam, J., J. Sheffield, X. Yuan, and E. F. Wood, 2014: Did a skillful prediction of sea surface temperatures help or hinder forecasting of the 2012 Midwestern US drought? *Environ. Res. Lett.*, **9**, 034005, <https://doi.org/10.1088/1748-9326/9/3/034005>.
- Karl, T. R., 1983: Some spatial characteristics of drought duration in the United States. *J. Appl. Meteor. Climatol.*, **22**, 1356–1366, [https://doi.org/10.1175/1520-0450\(1983\)022<1356:SSCODD>2.0.CO;2](https://doi.org/10.1175/1520-0450(1983)022<1356:SSCODD>2.0.CO;2).

- , F. Quinlan, and D. S. Ezell, 1987: Drought termination and amelioration: Its climatological probability. *J. Appl. Meteor. Climatol.*, **26**, 1198–1209, [https://doi.org/10.1175/1520-0450\(1987\)026<1198:DTAAIC>2.0.CO;2](https://doi.org/10.1175/1520-0450(1987)026<1198:DTAAIC>2.0.CO;2).
- , and A. J. Koscielny, 1982: Drought in the United States: 1895–1981. *J. Climatol.*, **2**, 313–329, <https://doi.org/10.1002/joc.3370020402>.
- Kellner, O., and D. Niyogi, 2015: Climate variability and the U.S. Corn Belt: ENSO and AO episode-dependent hydroclimatic feedbacks to corn production at regional and local scales. *Earth Interact.*, **19**, <https://doi.org/10.1175/EI-D-14-0031.1>.
- Kiladis, G. N., and H. F. Diaz, 1989: Global Climatic Anomalies Associated with Extremes in the Southern Oscillation. *J. Climate*, **2**, 1069–1090, [https://doi.org/10.1175/1520-0442\(1989\)002<1069:GCAAWE>2.0.CO;2](https://doi.org/10.1175/1520-0442(1989)002<1069:GCAAWE>2.0.CO;2).
- Kim, D., and J. D. Rhee, 2016: A drought index based on actual evapotranspiration from the Bouchet hypothesis. *Geophys. Res. Lett.*, **43**, 10 277–10 285, <https://doi.org/10.1002/2016GL070302>.
- Kirtman, B. P., and Coauthors, 2014: The North American Multimodel Ensemble: Phase-1 seasonal-to-interannual prediction; Phase-2 toward developing intraseasonal prediction. *Bull. Amer. Meteor. Soc.*, **95**, 585–601, [https://journals.ametsoc.org/search?f\\_0=author&q\\_0=Dughong+Min](https://journals.ametsoc.org/search?f_0=author&q_0=Dughong+Min).
- Klugman, M. R., 1978: Drought in the upper Midwest, 1931–1969. *J. Appl. Meteor. Climatol.*, **17**, 1425–1431, [https://doi.org/10.1175/1520-0450\(1978\)017<1425:DITUM>2.0.CO;2](https://doi.org/10.1175/1520-0450(1978)017<1425:DITUM>2.0.CO;2).
- Koster, R. D., M. J. Suarez, A. Ducharne, M. Stieglitz, and P. Kumar, 2000: A catchment-based approach to modeling land surface processes in a general circulation model: 1. Model structure. *J. Geophys. Res.*, **105**, 24 809–24 822, <https://doi.org/10.1029/2000JD900327>.
- Kumar, S., M. Newman, Y. Wang, and B. Livneh, 2019: Potential re-emergence of seasonal soil moisture anomalies in North America. *J. Climate*, **32**, 2707–2734, <https://doi.org/10.1175/JCLI-D-18-0540.1>.
- Liang, X., D. P. Lettenmaier, E. F. Wood, and S. J. Burges, 1994: A simple hydrologically based model of land surface water and energy fluxes for general circulation models. *J. Geophys. Res.*, **99**, 14 415–14 428, <https://doi.org/10.1029/94JD00483>.
- Livneh, B., and Coauthors, 2013: A long-term hydrologically based dataset of land surface fluxes and states for the conterminous United States: Update and extensions. *J. Climate*, **26**, 9384–9392, <https://doi.org/10.1175/JCLI-D-12-00508.1>.
- Lobell, D. B., M. J. Roberts, W. Schlenker, N. Braun, B. B. Little, R. M. Rejesus, and G. L. Hammer, 2014: Greater sensitivity to drought accompanies maize yield increase in the U.S. Midwest. *Science*, **344**, 516–519, <https://doi.org/10.1126/science.1251423>.
- Mallya, G., L. Zhao, X. C. Song, D. Niyogi, and R. S. Govindaraju, 2013: 2012 Midwest drought in the United States. *J. Hydrol. Eng.*, **18**, 737–745, [https://doi.org/10.1061/\(ASCE\)HE.1943-5584.0000786](https://doi.org/10.1061/(ASCE)HE.1943-5584.0000786).
- McKee, T. B., N. J. Doesken, and J. Kleist, 1993: The relationship of drought frequency and duration to timescales. Preprints, *Eighth Conf. on Applied Climatology*, Anaheim, CA, Amer. Meteor. Soc., 179–184.
- Messié, M., and F. Chavez, 2011: Global modes of sea surface temperature variability in relation to regional climate indices. *J. Climate*, **24**, 4314–4331, <https://doi.org/10.1175/2011JCLI3941.1>.
- Mishra, V., and K. A. Cherkauer, 2010: Retrospective droughts in the crop growing season: Implications to corn and soybean yield in the Midwestern United States. *Agric. For. Meteorol.*, **150**, 1030–1045, <https://doi.org/10.1016/j.agrformet.2010.04.002>.
- Mo, K. C., 2011: Drought onset and recovery over the United States. *J. Geophys. Res.*, **116**, D20106, <https://doi.org/10.1029/2011JD016168>.
- , and J. E. Schemm, 2008: Droughts and persistent wet spells over the United States and Mexico. *J. Climate*, **21**, 980–994, <https://doi.org/10.1175/2007JCLI1616.1>.
- , and B. Lyon, 2015: Global meteorological drought prediction using the North American multi-model ensemble. *J. Hydrometeorol.*, **16**, 1409–1424, <https://doi.org/10.1175/JHM-D-14-0192.1>.
- , and D. P. Lettenmaier, 2018: Drought variability and trends over the Central United States in the instrumental record. *J. Hydrometeorol.*, **19**, 1149–1166, <https://doi.org/10.1175/JHM-D-17-0225.1>.
- , L. N. Long, and J.-K. E. Schemm, 2012: Characteristics of drought and persistent wet spells over the United States in the atmosphere–land–ocean coupled model experiments. *Earth Interact.*, **16**, <https://doi.org/10.1175/2012EI000437.1>.
- Namias, J., 1983: Some causes of United States drought. *J. Appl. Meteor. Climatol.*, **22**, 30–39, [https://doi.org/10.1175/1520-0450\(1983\)022<0030:SCOUSD>2.0.CO;2](https://doi.org/10.1175/1520-0450(1983)022<0030:SCOUSD>2.0.CO;2).
- National Integrated Drought Information System, 2021: Midwest drought early warning system. NOAA, <https://www.drought.gov/dews/midwest#:~:text=What%20is%20Drought%20Early%20Warning,for%20decision%20makers%20and%20stakeholders>.
- NOAA/National Centers for Environmental Information, 2021: U.S. billion-dollar weather and climate disasters. <https://www.ncdc.noaa.gov/billions/>.
- Oladipo, E. O., 1986: Spatial patterns of drought in the interior plains of North America. *J. Climatol.*, **6**, 495–513, <https://doi.org/10.1002/joc.3370060505>.
- Oppedahl, D., 2018: Midwest agriculture’s ties to the global economy. Chicago Fed Letter 393, Federal Reserve Bank of Chicago, <https://www.chicagofed.org/publications/chicago-fed-letter/2018/393>.
- Otkin, J. A., M. Svoboda, E. D. Hunt, T. W. Ford, M. C. Anderson, C. Hain, and J. B. Basara, 2018: Flash droughts: A review and assessment of the challenges imposed by rapid-onset droughts in the United States. *Bull. Amer. Meteor. Soc.*, **99**, 911–919, <https://doi.org/10.1175/BAMS-D-17-0149.1>.
- Pendergrass, A. G., and Coauthors, 2020: Flash droughts present a new challenge for subseasonal-to-seasonal prediction. *Nat. Climate Change*, **10**, 191–199, <https://doi.org/10.1038/s41558-020-0709-0>.
- Peterson, T. C., and Coauthors, 2013: Monitoring and understanding changes in heat waves, cold waves, floods and droughts in the United States: State of knowledge. *Bull. Amer. Meteor. Soc.*, **94**, 821–834, <https://doi.org/10.1175/BAMS-D-12-00066.1>.
- Piechota, T. C., and J. A. Dracup, 1996: Drought and regional hydrologic variation in the United States: Associations with the El Niño–Southern Oscillation. *Water Resour. Res.*, **32**, 1359–1373, <https://doi.org/10.1029/96WR00353>.
- Poshtiri, M. P., and I. Pal, 2016: Patterns of hydrological drought indicators in major U.S. river basins. *Climatic Change*, **134**, 549–563, <https://doi.org/10.1007/s10584-015-1542-8>.
- Pryor, S. C., K. E. Kunkel, and J. T. Schoof, 2009: Did precipitation regimes change during the twentieth century? *Understanding Climate Change: Regional Climate Variability, Predictability, and Change in Midwestern USA*, S. Pryor Ed., Indiana University Press, 100–112.
- Rajagopalan, B., E. Cook, U. Lall, and B. K. Ray, 2000: Spatiotemporal variability of ENSO and SST teleconnections to

- summer drought over the United States during the twentieth century. *J. Climate*, **13**, 4244–4255, [https://doi.org/10.1175/1520-0442\(2000\)013<4244:SVOEAS>2.0.CO;2](https://doi.org/10.1175/1520-0442(2000)013<4244:SVOEAS>2.0.CO;2).
- Rasmusson, E. M., and J. M. Wallace, 1983: Meteorological aspects of the El Niño/Southern Oscillation. *Science*, **222**, 1195–1202, <https://doi.org/10.1126/science.222.4629.1195>.
- Rippey, B. R., 2015: The U.S. drought of 2012. *Wea. Climate Extremes*, **10**, 57–64, <https://doi.org/10.1016/j.wace.2015.10.004>.
- Ropelewski, C. F., and M. S. Halpert, 1986: North American precipitation and temperature patterns associated with the El Niño/Southern Oscillation (ENSO). *Mon. Wea. Rev.*, **114**, 2352–2362, [https://doi.org/10.1175/1520-0493\(1986\)114<2352:NAPATP>2.0.CO;2](https://doi.org/10.1175/1520-0493(1986)114<2352:NAPATP>2.0.CO;2).
- Ryu, J. H., M. D. Svoboda, J. D. Lenters, T. Tadesse, and C. L. Knutson, 2010: Potential extents for ENSO-driven hydrologic drought forecasts in the United States. *Climatic Change*, **101**, 575–597, <https://doi.org/10.1007/s10584-009-9705-0>.
- Schubert, S. D., M. J. Suarez, P. J. Pegion, R. D. Koster, and J. T. Bacmeister, 2004: On the cause of the 1930s dust bowl. *Science*, **303**, 1855–1859, <https://doi.org/10.1126/science.1095048>.
- Seager, R., 2007: The turn of the century North American drought: Global context, dynamics, and past analogs. *J. Climate*, **20**, 5527–5552, <https://doi.org/10.1175/2007JCLI1529.1>.
- , Y. Kushnir, M. Ting, M. Cane, N. Naik, and J. Miller, 2008: Would advance knowledge of 1930s SSTs have allowed prediction of the dust bowl drought? *J. Climate*, **21**, 3261–3281, <https://doi.org/10.1175/2007JCLI2134.1>.
- , and Coauthors, 2018: Whither the 100th Meridian? The once and future physical and human geography of America's arid-humid divide. Part I: The story so far. *Earth Interact.*, **22**, <https://doi.org/10.1175/EI-D-17-0011.1>.
- , J. Nakamura, and M. Ting, 2020: Prediction of seasonal meteorological drought onset and termination over the Southern Great Plains in the North American multimodel ensemble. *J. Hydrometeorol.*, **21**, 2237–2255, <https://doi.org/10.1175/JHM-D-20-0023.1>.
- Shah, D., and V. Mishra, 2020: Integrated drought index (IDI) for drought monitoring and assessment in India. *Water Resour. Res.*, **56**, e2019WR026284, <https://doi.org/10.1029/2019WR026284>.
- Shin, C.-S., B. Huang, P. A. Dirmeyer, S. Halder, and A. Kumar, 2020: Sensitivity of U.S. drought prediction skill to land initial states. *J. Hydrometeorol.*, **21**, 2793–2811, <https://doi.org/10.1175/JHM-D-20-0025.1>.
- Shukla, S., and A. W. Wood, 2008: Use of a standardized runoff index for characterizing hydrologic drought. *Geophys. Res. Lett.*, **35**, L02405, <https://doi.org/10.1029/2007GL032487>.
- Slivinski, L. C., and Coauthors, 2019: Towards a more reliable historical reanalysis: Improvements for version 3 of the Twentieth Century Reanalysis system. *Quart. J. Roy. Meteor. Soc.*, **145**, 2876–2908, <https://doi.org/10.1002/qj.3598>.
- Soulé, P. T., 1992: Spatial patterns of drought frequency and duration in the contiguous USA based on multiple drought event definitions. *Int. J. Climatol.*, **12**, 11–24, <https://doi.org/10.1002/joc.3370120103>.
- State of Illinois Department of Natural Resources, 2013: The drought of 2012: A report of the Governor's drought response task force. 96 pp., <https://www2.illinois.gov/dnr/WaterResources/Documents/TheDroughtOf2012.pdf>.
- Svoboda, M., and Coauthors, 2002: The Drought Monitor. *Bull. Amer. Meteor. Soc.*, **83**, 1181–1190, <https://doi.org/10.1175/1520-0477-83.8.1181>.
- Trenberth, K. E., G. W. Branstator, and P. A. Arkin, 1988: Origins of the 1988 North American drought. *Science*, **242**, 1640–1645, <https://doi.org/10.1126/science.242.4886.1640>.
- U.S. Census Bureau, 2021: Census regions and divisions of the United States. [https://www2.census.gov/geo/pdfs/maps-data/maps/reference/us\\_regdiv.pdf](https://www2.census.gov/geo/pdfs/maps-data/maps/reference/us_regdiv.pdf).
- U.S. Department of Agriculture Midwest Climate Hub, 2021: Agriculture in the Midwest. <https://www.climatehubs.usda.gov/hubs/midwest/topic/agriculture-midwest>.
- U.S. Department of Agriculture National Agriculture Statistics Service, 2019: Corn: Production acreage by county. [https://www.nass.usda.gov/Charts\\_and\\_Maps/Crops\\_County/cr-pr.php](https://www.nass.usda.gov/Charts_and_Maps/Crops_County/cr-pr.php).
- Walsh, J. E., M. B. Richman, and D. W. Allen, 1982: Spatial coherence of monthly precipitation in the United States. *Mon. Wea. Rev.*, **110**, 272–286, [https://doi.org/10.1175/1520-0493\(1982\)110<0272:SCOMPI>2.0.CO;2](https://doi.org/10.1175/1520-0493(1982)110<0272:SCOMPI>2.0.CO;2).
- Wang, A., T. J. Bohn, S. P. Mahanama, R. D. Koster, and D. P. Lettenmaier, 2009: Multimodel ensemble reconstruction of drought over the continental United States. *J. Climate*, **22**, 2694–2712, <https://doi.org/10.1175/2008JCLI2586.1>.
- Wang, D., M. Hejazi, X. Cai, and A. J. Valocchi, 2011: Climate change impact on meteorological, agricultural, and hydrological drought in central Illinois. *Water Resour. Res.*, **47**, W09527, <https://doi.org/10.1029/2010WR009845>.
- Wang, R., L. C. Bowling, and K. A. Cherkauer, 2016: Estimation of the effects of climate variability on crop yield in the Midwest USA. *Agric. For. Meteorol.*, **216**, 141–156, <https://doi.org/10.1016/j.agrformet.2015.10.001>.
- Ward, J. H., Jr., 1963: Hierarchical grouping to optimize an objective function. *J. Amer. Stat. Assoc.*, **58**, 236–244, <https://doi.org/10.1080/01621459.1963.10500845>.
- Xia, Y., M. B. Ek, C. D. Peters-Lidard, D. Mocko, M. Svoboda, J. Sheffield, and E. F. Wood, 2014: Application of USDM statistics in NLDAS-2: Optimal blended NLDAS drought index over the continental United States. *J. Geophys. Res. Atmos.*, **119**, 2947–2965, <https://doi.org/10.1002/2013JD020994>.
- Yuan, X., and E. F. Wood, 2013: Multimodel seasonal forecasting of global drought onset. *Geophys. Res. Lett.*, **40**, 4900–4905, <https://doi.org/10.1002/grl.50949>.
- Zhuang, Y., A. Erfanian, and R. Fu, 2021: Dryness over the U.S. Southwest, a springboard for cold season Pacific SST to influence warm season drought over the U.S. Great Plains. *J. Hydrometeorol.*, **22**, 63–76, <https://doi.org/10.1175/JHM-D-20-0029.1>.